Late Cretaceous to early Paleogene foraminiferal biozones in the Tibetan Himalayas, and a pan-Tethyan foraminiferal correlation scheme

Marcelle K. BouDagher-Fadel[1,3], G. David Price[1], Xiumian Hu[2], Juan Li[2]

[1]*Department Earth Sciences, UCL, Gower Street, London, WC1E 6BT, UK*

[2] *School of Earth Sciences and Engineering, Nanjing University, Xianlindadao 163, Nanjing, 210023, China*

Email: m.fadel@ucl.ac.uk

Abstract: This investigation of Upper Cretaceous and lower Paleogene sediments from the Tibetan Himalayas, based on three stratigraphic sections from the southern margin of Asian Plate and nine sections from the northern Indian Plate margin, provides the first high resolution biostratigraphic description of the region. The sedimentary successions from these two plate margins evolved during the following depositional stages, which we here divide into eleven new biozones (TLK2-3 and TP1-9); (i) an outer neritic stage from the Coniacian to the Maastrichtian, dominated by keeled planktonic foraminifera (PF), such as *Globotruncana* (TLK2); (ii) a latest Maastrichtian forereef assemblage dominated by *Lepidorbitoides*, *Omphalocyclus* and *Orbitoides* (TLK3); (iii) an early Paleocene, intermittently occurring backreef/shallow reefal warm environment with benthic assemblages dominated by small miliolids and rotaliids, such as *Daviesina* and *Lockhartia* (TP1-2); (iv) a late Paleocene-early Eocene, shallow reefal environment dominated by warm water forms, such as *Alveolina, Assilina* and *Nummulites* (TP3-7); (v) a depositional stage showing a slight deepening of the reef, with forereef assemblages, lasting until the end of the Ypresian (TP8); (vi) a final, early Lutetian depositional stage characterised by the complete disappearance of the larger benthic foraminifera (LBF) and their reefal environment, which was replaced by PF assemblages with intense reworking of pelagic facies triggered by the tectonics of the India-Asia collision (TP9). During the course of this study two unnamed species have been identified and described, *Lepidorbitoides* sp. A and *Discocyclina* sp. A, from the Xigaze forearc basin. The high resolution depositional and biostratigraphic scheme defined here for the southern Himalayan region gives greater insight into the general evolution of this globally

important tectonic region. We have confirmed earlier observations that many LBF forms appear about 1 Ma later in the eastern part of Tethys than they do in the west, reflecting their previously inferred gradual eastern paleogeographic migration. Additionally, this study has allowed us to refine the biostratigraphic ranges of some LBF of the Eastern Tethys, and for the first time to exactly correlate these Eastern Tethyan zones with the Shallow Benthic Zones (SBZs) of the Western Tethys.

INTRODUCTION

The Upper Cretaceous and lower Paleogene sedimentary succession from the Himalayan region records the depositional history of the margins of the Indian and Asian plates before and after their tectonic collision. During this period the Indian Plate drifted rapidly northward in the direction of the Asian Plate (see text-fig.1). Plate reconstructions show that, at this time, the margins of the Indian and Asian plates lay near tropical latitudes, and so favoured the formation of reefal and related limestone complexes, which are frequently characterised by being largely composed of larger benthic foraminifera (LBF), planktonic foraminifera (PF), corals and algae. These fossil forms are used as biostratigraphic and paleoenvironmental indicators to assist in understanding the geological history of these regions.

The material we describe in this study was obtained from a systematic sampling of nine sections from the Gamba, Zhepure Shanpo and Longjiang areas (Tingri) (see text-figs 2), which were deposited on the northern margin of the Indian Plate, and three sections from the Cuojiangding (Zhongba), Dajin (Burang) and Dajiweng (Gar) (text-figures 3-14), deposited along the southern margin of Asian Plate. The sections have ages ranging from Late Cretaceous (Coniacian) to early middle Eocene (Lutetian).

In this paper, we develop a high resolution Late Cretaceous to early Eocene biozonation scheme, based chiefly on foraminiferal assemblages, for southern Tibet. The biozonations erected here are compared with those already described by Zhang, Willems and Ding (2013) from the Paleocene – early Eocene of Tibetan Tethyan Himalaya, and are based on the stratigraphic first occurrences of index foraminifera,

and on the changes in the foraminiferal facies throughout the sections. However, the use of Zhang, Willems and Ding (2013) of SBZs needs to be reconsidered as their age assignment of SBZ 2, 3, 4, 5 and 6 is not in agreement with Serra-Kiel et al. (1998). In the shallow carbonate facies, LBF dominate assemblages. However in the deeper water carbonates, PF facies dominate, and the existing well-established biostratigraphic ranges of the PF (see BouDagher-Fadel, 2013a) are used to assign the ages of the different sections. In this paper, we define eleven informal biozones: two biozones (TLK2, TLK3) for the Late Cretaceous; four (TP1-TP4) for the Paleocene; and five (TP5-TP9) for early to middle Eocene (see text-fig. 15).

In the course of this study we have also identified two unnamed species, *Lepidorbitoides* sp. A and *Discocyclina* sp. A, from the Xigaze forearc basin. The details of these species are given in the Appendix.

LBFs are highly specialised forms (see BouDagher-Fadel 2008), and are therefore highly sensitive to their environment. As a result, their distribution in a sedimentary section provides considerable insight into the paleoenvironmental evolution of the plate margins. We are able, therefore, to analyse the paleoenvironmental changes that occurred during deposition of the carbonate succession of the Indian and Asian Plates margins during the Late Cretaceous, Paleocene and early Eocene. The PF facies, and their co-occurrence in some samples with LBF forms, provide a rare opportunity for correlating the biostratigraphic framework of these two groups. This not only has allowed us to refine the biostratigraphic ranges of some LFB forms, but also extends our ability to correlate them with the proposed shallow benthic zones (SBZ) of the Western Tethys, thereby producing for the first time a pan-Tethyan LBF biozonation scheme (see text-fig. 16).

PREVIOUS STUDIES OF TETHYAN LBF BIOZONES

By the late 1920s, LBF had become the preferred fossil group for Paleogene biostratigraphy in the Tethyan area, and regional biostratigraphic zonations were developed for many parts of the world, including for example, the Paleogene sequences of NE India (Jauhri and Agarwal, 2001), the Neogene

sequences of the Indo-Pacific region (van der Vlerk and Umbgrove 1927; Chapronière 1984; Adams 1984; BouDagher-Fadel and Banner 1999; BouDagher-Fadel 2008) and the Cenozoic of northern Oman (Racey 1995). The study of the evolutionary lineages and stratigraphic distribution of the Mediterranean orthophragminids, alveolinids and nummulitids led Serra-Kiel et al. (1998) to propose 20 Paleocene–Eocene SBZ for the Western Tethys. However, these western zonations have only recently (Afzal et al. 2011) been linked or partially correlated with those in Eastern Tethys, and so there has been, thus far, no pan-Tethyan correlation scheme.

What is now southern Tibet was, in the Late Cretaceous and early Paleogene, paleogeographically located at the margins of eastern Tethyan Ocean, and was the site for the deposition of large volumes of shallow water marine carbonates, which accumulated between deeper water sediments of earliest Late Cretaceous and the earliest middle Eocene ages. During this time, the variations in the different foraminiferal assemblages hold the key to understanding the paleoenvironmental development of the region, and the timing of the India-Asia collision. However, although some isolated occurrences of LBF have been reported in the last four decades (He *et al.* 1976; Zhang 1988; Wan 1990, 1991; Najman et al. 2010; Willems et al. 1996; Zhang et al. 2012; Zhang, Willems and Ding 2013), the Tibetan foraminifera of the Late Cretaceous-early Paleogene still remain poorly described. This study remedies this shortcoming, and is based on a detailed high resolution biostratigraphical study of over 700 thin sectioned samples from 12 outcrop sections, 9 of which are from Gamba, Zhepure and Longjiang in Tingri area in northern Indian margin, and 3 sections are from Cuojiangding (Zhongba), Dajin (Burang) and Dajiweng (Gar) in the southern margin of Asian Plate (see Figs 2 and 3). We have been able to compare our findings with previous attempted systematic studies from the deep-water Cretaceous facies in the eastern part of the Tethyan Himalaya (Wan 1987, 1992; Li et al. 2009) and the shallow-water Paleocene-Eocene facies of Tingri and Gamba areas in the southern Tethyan Himalaya (Wendler et al. 2009, 2011; Zhang et al. 2012; Li et al. 2014).

GEOLOGIC SETTING, MATERIALS AND METHODS

The Indus-Yarlung suture zone (text-fig. 2) delineates the east-west trending contact between the Indian and Asian Plates for over 2500 km (e.g. Gansser 1980). The Cretaceous Xigaze Forearc basin is considered to be the forearc to the southern active margin of the Asian Plate, including the abyssal sediments at the base (Chongdui Formation), deep-sea turbidites (Ngamring Formation), and shelf and deltaic facies at the top (Padana Formation) (Einsele et al. 1994; Dürr 1996; Wang et al. 2012; An et al. 2014).

In the Cuojiangding-Dajin-Dajiweng area, the uppermost Cretaceous Padana and Qubeiya formations, were deposited in deltaic to inner shelf environments, and represent the final filling stage of the Xigaze Forearc basin (An et al. 2014; Wang et al. 2014). Sediments in the Xigaze Forearc basin were discomformably overlain by the Cuojiangding Group (Quxia and Jialazi formations), deposited in fan-delta environments during the Paleocene-earliest Eocene, which are interpreted to be the syn-collisional basin deposition in front of the proto-Himalayan Range (Hu et al., submitted). North of the Xigaze Forearc basin, and located in the southern part of the Lhasa Block (text-fig. 2), the Gangdese Arc is composed of Jurassic to Cretaceous granitoids and Cretaceous to Cenozoic terrigenous and volcanic rocks (e.g. Zhu et al. 2011).

Directly south of the Indus-Yarlung suture zone is the Tibetan Tethyan Himalaya, once belonging to the northern margin of Indian Plate prior to the India-Asia collision, that comprises a southern and a northern zone (Ratschbacher et al. 1994). The southern Tethyan Himalaya includes platform carbonates and diverse terrigenous units of Paleozoic to Eocene age (Willems et al. 1996; Jadoul Berra and Garzanti 1998; Hu et al. 2012), whereas the northern Tethyan Himalaya is dominated by Mesozoic to Paleogene outer shelf, continental slope and rise deposits (Hu et al. 2012).

During the earliest Cretaceous, the northern margin of India was situated at middle latitudes in the southern hemisphere (Patzelt, Wang and Appel 1996), while the Lhasa block was in low latitudes of the northern hemisphere. India rifted from Gondwana in the Early Cretaceous, and drifted northwards

during Late Cretaceous-early Paleogene (e.g. Hu et al. 2010; and references therein), to collide with the Lhasa Block (Asian Plate) around the Paleocene-Eocene boundary (56 ± 5 Ma; see reviews by Najman et al. 2010; Hu et al. 2012; Zhang et al. 2012), however currently the exact timing of the India-Asia collision remains debated.

The material described in this paper is from the Jiubao, Zhepure Shanpo/Zongshan, Jidula, Zongpu and Enba formations, from locations on the southern margin of the eastern Tethyan sea (see text-fig. 2; Hu et al. 2012), with the lithostratigraphy followed by Hu et al. (2012), and from the Qubeiya, Quixia, Jialazi, Dajin formations from locations on the northern margin of the eastern Tethys (see Ding et al. 2005; Hu et al. 2013). We studied nearly 700 samples (mainly thin sections) of outcrop sections sampled by Xiumian Hu, with help from his students, in the years of 2006-2013. The samples were mainly carbonates, and they were virtually all fossiliferous. Most thin sections were found to be very rich in LBF and algae.

PF are dominant in the Upper Cretaceous Jiubao Formation and the lower middle Eocene Enba Formation. The co-occurrence of LBF with PF at some levels of the lower Eocene is vital for the correlation and refining the biostratigraphy of some of the long-ranging LBF. All the LBF were identified and the main species are plotted in text-fig. 16, in relation to the proposed foraminiferal biozonations. In our definitions of stratigraphic ranges, we primarily use the PF zonal scheme of BouDagher-Fadel (2013a), which is tied to the time scale of Gradstein et al. (2012). This scheme is developed from the calibration of the N-zonal scheme of Blow (1979), and the M-zonal scheme of Berggren (1973), which has been recently revised by Wade et al. (2011). In this paper, the PF zonal scheme of BouDagher-Fadel (2013a) and the shallow benthic foraminiferal zones (SBZ) for the Paleogene are correlated to our new biozonation scheme, based the observed assemblages of LBF and/or PF, and so provides for the first time a pan-Tethyan correlation (see text-fig. 16). Sampling intervals of the outcrops were sufficiently fine scale to validate the application of the proposed biostratigraphic scheme for the Upper Cretaceous to the lowest middle Eocene, and to suggest its applicability to coeval

carbonate successions from other localities. The figured specimens are deposited in the School of Earth Sciences and Engineering, Nanjing University (China).

OCCURRENCES OF FORAMINIFERA IN THE STUDIED SECTIONS

The occurrences of the foraminifera in the 12 sections of Gamba, Zhepure, Longjiang and Xigaze Forearc Basin are plotted against the stratigraphic logs and correlated with the Tibetan formations and the Tibetan foraminifera zones (text-figs 4-14). Their distribution allow the understanding of the chronostratigraphy and the paleoenvironmental deposition of the Tethyan Himalayas and the Xigaze forearc basin.

The Cretaceous planktonic foraminiferal zones (TLK2 a-c) occur in Jiubao (text-fig. 3) and Gelamu (text-fig. 6) sections in the Gamba and Zhepure areas respectively. The foraminiferal distribution indicates a disconformity at the lowest bed of the Zhepure Shanpo Formation in the Gelamu section, in the lower part of TLK2d, where 2.1 Million of years of early Maastrichtian deposits (Maastrichtian 1, see BouDagher-Fadel, 2013) are eroded or missing. This is confirmed by the first occurrence of *Globotruncanita conica* and *Abathomphalus mayaroensis* confirming the presence of only the upper deposits of TLK2d in the section.

The appearance of the larger benthic foraminifera (e.g. *Omphalocyclus macroporus*) indicates the beginning of the shallow water benthic foraminifera (TLK3) in Gelamu, Jidula (text-fig. 4) and Cuojiangding (text-fig. 12) sections.

The occurrences of the Paleogene larger benthic foraminifera of the Jidula, Zongpu, Zhepure Shanpo formations in the Tethyan Himalayas and the Quxia, Jalazi, Dajin and Dajiweng formations in the Xigaze forearc Basin are correlated with the Tibetan zones (TP1-TP8) (text-figs 4-14). In the Qumiba section, Tingri area, the older bed TP2 of the Zongbu Formation thrust the younger bed TP7, while a disconformity occur between TP2 and TP6 as confirmed by the foraminiferal distribution (text-fig. 9). In Naiqiong section the older Zongpu Formation thrust over the Zhaguo and Enba formations (text-fig.10).

In the Cuojiangding, Zhongba area, the foraminiferal occurrences indicate a disconformity between the Cretaceous Qubeiya Formation and the Paleogene Quxia Formation, where TP1 foraminiferal biozone are missing (text-fig. 12).

The TP8 benthic foraminifera are replaced abruptly by the planktonic foraminifera of the Enba Formation in Qumiba and Naiqiong sections (Tingri area) (text-figs 9-10). Foraminiferal occurrences in the Zongpubei section in Gamba and Naiqiong section in Tingri indicate a disconformity between the Zongpu and Enba formations where TP8 foraminiferal biozones are missing. The Enba Formation in Longjiang section was mainly composed of quartzarenite and shale which were mainly barren of diagnostic foraminifera.

DEFINITION OF THE TIBETAN FORAMINIFERAL BIOZONES (TLK and TP BIOZONES)

The carbonate successions described here evolved during the following six depositional stages, which we divide into eleven biozones (TLK2-3 and TP1-9, see text-fig. 16):

- An outer neritic stage from the Coniacian to Maastrichtian dominated by keeled planktonic foraminifera, such as *Globotruncana*. (TLK2) [N.b. The Lower Cretaceous biozone TLK1 is the subject of a different study, BouDagher-Fadel et al. (in preparation)].
- A latest Maastrichtian forereef assemblage dominated by *Lepidorbitoides*, *Omphalocyclus* and *Orbitoides* species (TLK3).
- An early Paleocene, intermittently occurring backreef/shallow reefal environment where observed benthic assemblages were dominated by small miliolids and rotaliids such as *Daviesina* and *Lockhartia* (TP1-2). The nummulitid *Ranikothalia* makes its first appearance in TP1c (late Selandian).
- A late Paleocene – early Eocene, shallow reefal environment dominated by warm water forms such as *Alveolina, Assilina* and *Nummulites* (TP3-7).
- A depositional stage showing a slight deepening of the reef, with forereef assemblages lasting until the end of the Ypresian (TP8).

- A final depositional stage characterised by the complete disappearance of the larger benthic foraminifera and their reefal environment. They were replaced by planktonic foraminiferal assemblages with intense reworking of pelagic facies related to tectonic changes of the India-Asia collision (TP9).

In the detail, foraminiferal distribution in each section are listed in Apperndix 2. The biozones are characterized as follows:

Biozone TLK2 (Coniacian – Maastrichtian 2, 89.8 – 70 Ma, Indian Plate: Jiubao section (text-fig. 3) in Gamba, Gelamu section (text-fig. 8) in Tingri). It corresponds to the Jiubao Formation in the Gamba and Tingri areas, and the lower part of the Zongshan in the Jidula section of the Gamba (text-fig. 15). TLK2 represents the outer neritic phase of the Late Cretaceous where planktonic foraminifera dominate the foraminiferal assemblages. The lower boundary of biozone TLK2 is defined by the lowest occurrence of *Concavatotruncana concavata*. The upper boundary of TLK2 is defined by the lowest occurrence of *Omphalocyclus macroporus*. In the absence of *C. concavata*, the first occurrence of *Dicarinella primitiva* defines the lowest boundary of TLK2. In the absence of *O. macroporus*, the lowest occurrence of *Lepidorbitoides* sp. A defines the upper boundary of TLK2. TLK2 is divided into 4 subdivisions, TLK2a-TLK2d which are equivalent to PF zones Coniacian 1 to Maastrichtian 2 (see BouDagher-Fadel 2013a,b):

- Subzone TLK2a (Coniacian, 89.8-86.3 Ma, based on the presence of *Dicarinella primitiva, Concavatotruncana concavata* and *Contusotruncana fornicata*) was studied from the Jiubao section in Gamba (text-fig. 3). The assemblage is dominated by *Concavatotruncana concavata, Contusotruncana fornicata, Globotruncana lapparenti, Dicarinella primitiva, Marginotruncana coronata* and *M. pseudolinneiana* (Plate 2, Fig. 1A). The lower boundary of the subzone is defined by the lowest occurrence of *C. concavata* (Plate 2, Fig. 2) and by the last appearance of *D. primitiva*;
- Subzone TLK2b (Santonian 86.3-83.6 Ma, based on the presence of *Concavatotruncana asymetrica* and *C. concavata*) was studied in the Jiubao section (text-Fig. 3). The assemblages

include *Concavatotruncana asymetrica*, *Cv. concavata*, *Globotruncana arca*, *Ga linneiana*, *Contusotruncana fornicata*, *Marginotruncana coronata*. The lower boundary of the subzone is defined by the lowest occurrence of *Cv. asymetrica*. Its upper boundary is defined by the highest occurrence of *Cv. concavata* (Plate 2, Fig. 2);

- Subzone TLK2c (Campanian, 83.6-72.1 Ma, based on the presence of *Globotruncanita stuartiformis* and *Radotruncana subspinosa*) was studied in the Jiubao section (text-fig. 3) in Gamba and the Gelamu section (text-fig. 6) in Tingri. The assemblage is dominated by by *C. fornicata, Ga linneiana, Radotruncana subspinosa, Globotruncanita elevata, Gta stuartiformis*. The lower boundary of the subzone is defined by the appearance of *Gta stuartiformis*. Its upper boundary is defined by disappearance of *R. subspinosa*;
- Subzone TLK2d (lower to middle Maastrichtian, 72.1-67.0 Ma, based on the presence of *Globotruncanita stuarti, Gta conica* and *Kuglerina rotundata*) was studied in the Gelamu (text-fig. 6) and the Zhepure Shanpo (text-fig. 7) sections in Tingri. TLK2d assemblage include *Globotruncanita stuarti, Gta pettersi, Gta conica*, *Globotruncana linneiana, Abathomphalus mayaroensis* and *Kuglerina rotundata*. The lower boundary of the subzone is defined by the lowest occurrence of *K. rotundata* in Zhepure Shanpo section. The lower part of TLK2d (Maastrichtian 1) is eroded or missing in the Gelamu section where the first occurrence of *Gta conica* and *A. mayaroensis* indicates an upper TLK2d (Maastrichtian 2, see BouDagher-Fadel, 2013). The upper boundary of TLK2 is defined by the lowest occurrence of *Omphalocyclus macroporus* and *Lepidorbitoides* sp. A.

Biozone TLK3: (Maastrichtian 3, 67.0-66.0 Ma, Indian Plate: Jidula section (text-fig. 4) in Gamba, Gelamu (text-fig. 6) and Zhepure Shanpo (text-fig. 7) sections in Tingri; Asian Plate: Cuoajangdiung section (text-fig. 12) in Zhongba area). It corresponds to the upper part of the Zongshan Formation in the Jidula section of the Gamba area, the lower part of the Zhepure Shan Formation in the Zhepure Shanpo section of the Tingri area, and to the Qubeiya Formation in the Cuojiangding area of the Zhongba area (see text-fig. 16). TLK3 represents the shallow open marine reefal facies of the late Maastrichtian and it is equivalent to the PF zone Maastrichtian 3 (see BouDagher-Fadel 2013a,b). The assemblages of

the LBF are dominated by *Lepidorbitoides* sp. A (Plate 1, Figs 1-8), *L. blanfordi, L. minor* (Plate 2, Fig. 3), *L. zhongbaensis, L. gangdiscus* and *Omphalocyclus macroporus, Orbitoides medius* (Plate 2, Fig. 4). Planktonic foraminifera are rare to bsent. They are represented by *Globotruncana arca, Globotruncanita stuarti, Abathomphalus mayaroensis, Kuglerina rotundata, Globotruncanita conica* and *Racemiguembelina intermedia.* This subzone is defined by the full biostratigraphic range of *Omphalocyclus macroporus* (Plate 2, Fig. 5). In the absence of *O. macroporus*, the first appearance of *Lepidorbitoides* sp. A defines the lower boundary of TLK3 (e.g. Cuoajangdiung section (text-fig. 12) in Zhongba area).

Biozone TP1: (Danian-Selandian, 66.0-59.2 Ma, Indian Plate: Jidula section (text-fig. 4) in Gamba area, Zhepure Shanpo section (text-fig. 7) and Shenkeza section (text-fig. 8) in Tingri area; Asian Plate: Cuoajangdiung section (text-fig. 12) in Zhongba area). It corresponds to the Jidula Formation in the Gamba and Tingri areas (see text-fig. 15) and to the Zhepure Shan Formation in the Tingri area. The Jidula Formation has previously been described as being composed mainly of pure quartz sandstone barren of fossils (see Zhang, Willems and Ding 2013). However, within the Jidula Formation, there are some intermittently occurring, interbedded or lens-shape limestones in the Gamba and Tingri area (Willems and Zhang 1993; Wan et al. 2002). These limestones have been sampled as part of this study, and are found to be transgressional from lagoonal to open marine shallow reefal facies of early Paleocene (Danian –Selandian) age, which are used to define Biozone TP1. The lower boundary of this TP1 is defined by the first occurrence of *Lockhartia conditi*, while the lowest occurrence of *Miscellanea yvettae* serve to define the upper boundary of this biozone. TP1 can be divided into three subzones TP1a-c which are equivalent (see text-fig. 16) to the Danian and Selandian (P1-P4b, see BouDagher-Fadel, 2013a,b, or SBZ1 to the lower part of SBZ3a):

- Subzone TP1a (Danian, P1-P2, 66.0-61.6 Ma, corresponds to SBZ1, based on the presence of *Lockhartia conditi* and *Orbitosiphon* sp. A) was studied in Jidula section (text-fig. 4), Zhepure Shanpo section (text-fig. 7) and Shenkeza section (text-fig. 8). The assemblages are mainly poorly preserved and dominated by few small benthic foraminifera such as small rotaliids, *Rotorbinella skourensis, Laffitteina bibensis, Textularia* spp., small miliolids, *Daviesina* sp. A,

Vacuovalvulina sp., *Orbitosiphon* sp. A, and *Lockhartia conditi*. Planktonic foraminifera are scarce, represented by small fragile forms such as *Globanomalina* sp. and *Parasubbotina pseudobulloides.* TP1a is defined by the first appearance of *L. conditi* (Plate 2, Fig. 9) and the lowest occurrence of *Lockhartia haimei*. TP1a represents the lagoonal phase of the Jidula Formation in Gamba area and and Tingri areas (see text-figs 15, 17).

- Subzone TP1b (lower Selandian, P3, 61.6-60.0 Ma, corresponds to the lower part of SBZ2, based on the presence of *Lockhartia haimei, Rotalia dukhani* and *Orbitosiphon punjabensis*) was studied from Jidula section (text-fig. 4) Zhepure Shanpo section (text-fig. 7), and Shenkeza sextion (text-fig. 8). The assemblages are dominated by the benthic foraminifera *Lockhartia haimei, L. conditi, Orbitosiphon punjabensis, Rotalia dukhani, Rotorbinella skourensis*. The planktonic foraminifera are present but rare. They are represented by *Igorina pusilla* and *Parasubbotina pseudobulloides.* TP1b is defined by the first appearance of *O. punjabensis* (Plate 2, Fig. 10) and *L. haimei* and by the lowest occurrence of *Daviesina langhami*. According to Zhang, Willems and Ding (2013) the dominant LBFs at the base of SBZ2 are *Rotorbinella skourensis, Lockhartia retiata,* and *Daviesina danieli.* TP1b represents the shallow open marine backreefal environment found in the Jidula Formation in Gamba area, the Zongpu and the Zhepure Shan formations in Tingri area (see text-figs 15, 17).
- Subzone TP1c (late Selandian, P4a, 60.0-59.2 Ma, corresponds to the upper part of SBZ2 and the lower part of SBZ3, based on the presence of *Daviesina langhami, Ranikothalia bermudezi* and *Lockhartia haimei*) was studied from Jidula section (text-fig. 4) and Shenkeza section (text-fig. 8). The assemblages include *Ranikothalia bermudezi, Lockhartia haimei, L. conditi* (Plate 2, Fig. 9), *L. cushmani, Daviesina langhami* (Plate 2, Fig. 8) and *Subbotina velascoensis.* The lower boundary of TP1c is defined by the first appearance of *Daviesina langhami* (Plate 2, Fig. 8) and the upper boundary is defined by the lowest occurrence of *Miscellanea yvettae*. TP1c represents the open marine shallow reefal waters of the Zongpu Formation in Gamba area and the Zhepure Shan Formation in Tingri area (see text-figs 15, 17).

***Biozone TP2*:** (lower Thanetian, P4b, 59.2-57.0 Ma, corresponds to the upper part of SBZ3 zone, based on the occurrence of *Miscellanea yvettae, M. julietta, Keramosphaerinopsis haydeni* and *Ranikothalia sindensis*) was studied from the Jidula section (text-fig. 4), the Zongpubei section (text-fig. 5) in Gamba area and the Shenkeza (text-fig. 8) section and the Qumiba (text-fig. 9) section in Tingri area and from the Cuojiangding (text-fig. 12) section in Zhongba area. The assemblages include *Miscellanea yvettae, M. julietta, Miscellanites minutus, Ranikothalia bermudezi, Daviesina khatiyahi, D. langhami, Lockhartia diversa, Orbitosiphon punjabensis* (Plate 2, Fig. 10), *Lockhartia haimei, L. cushmani, Keramosphaerinopsis haydeni* and *Ranikothalia sindensis* (Plate 1, Figs 10, 11B). TP2 is defined by the first appearance of *M. yvettae* (Plate 1, Figs 9, 10, 13), *Ranikothalia sindensis* and the last occurrence of *R. bermudezi* and *D. khatiyahi*. In the absence of *Miscellanea* spp., *Keramosphaerinopsis haydeni* is designated here as an index fossil to TP2 in the Shenkeza section in Tingri area. Zhang, Willems and Ding (2013) recorded *Keramosphaerinopsis haydeni* as an index fossil for SBZ3. However, in their definition of SBZ 3 they state: "*Keramosphaerinopsis haydeni* can be taken as an index fossil for SBZ 3 owing to its high abundance and limited biostratigraphic range", but they also recorded its appearance in (their) SBZ 4, thereby invalidating their scheme. In this study, *K. haydeni* is only found in the Shenkeza section in the upper part of SBZ3 and was never found in SBZ4. TP2 assemblages were deposited in a normal marine reefal environment in the Zongpu Formation of Gamba and Tingri. However, TP2 assemblages from the Zhepure Shan Formation of Tingri and the Quxia Formation of Zhongba were deposited in a backreefal environment (see text-figs 15, 17).

Biozone TP3: (Middle Thanetian, P4c, 57.0-56.4 Ma, corresponds to SBZ4 based on the occurrence of *Discocyclina sella, Nummulites heberti, Glomalveolina levis* and *Aberisphaera gambanica*) was studied from the Zongpubei section in Gamba area (text-fig. 5), the Shenkeza section in Tingri area (text-fig. 8) and Cuojiangding section in Zhongba area (text-fig. 12). The assemblages in Gamba and Tingri include *Lockhartia conditi, L. haimei, Daviesina langhami, Ranikothalia sindensis.* TP3 is defined by the stratigraphic range of *Glomalveolina levis* in Gamba area and of *Aberisphaera gambanica* (Plate 2, Fig. 20) in Tingri area. *Lockhartia conditi, Daviesina langhami, Lockhartia haimei, Lockhartia cushmani* and. On the other hand, the assemblages of the Zongba area include *Nummulites heberti, Ranikothalia*

sindensis, R. sahnii, R. thalica (Plate 1, Fig.11A), *Miscellanea yvettae, Discocyclina regularis, D. sella, D. ramaraoi, D. tenuis, D. ranikotensis* and *Assilina subspinosa* (Plate 1, Fig. 22). Rare planktonic foraminifera (e.g., *Pseudomenardella ehrenbergi,* Plate 1, Fig. 20) are also present. The lower boundary of TP3 is defined in Zongba is defined by the first appearance of *N. heberti* (Plate 1, Fig. 12) or *D. sella* (Plate 2, Fig. 19B) and the upper boundary by the lowest occurrence of *Discocyclina* sp. A. TP3 assemblages of the Zongpu Formation were deposited in a shallow reefal environment, while those of the Jialazi Formation in a reefal to forereef environment. On the other hand, TP3 assemblages from Zhepure Shan Formation indicate a backreef setting during this time in the Zhepure area. (see text-figs 15, 17).

Biozone TP4: (Late Thanetian, P5a, 56.4-56.0 Ma, SBZ5 and the earliest part of SBZ6 based on the occurrence of *Alveolina vredenburgi, A. aramaea, Miscellanea miscella* and *Assilina dandotica*) was studied from the Zongpubei (test-fig. 15) section, Shenkeza (text-fig. 8) section and Cuojiangding (text-fig. 12) section and Dajin (text-fig. 13) section. The Gamba and Tingri areas assemblages include *Alveolina vredenburgi, A. aramaea Miscellanea miscella, Lockhartia diversa L. haimei, Ranikothalia sindensis, Daviesina langhami* and *Orbitosiphon punjabensis.* TP4 is defined by the biostratigraphic ranges of *M. miscella* (Plate 2, Fig. 11). Zhang, Willems and Ding (2013) recorded the appearance of *M. miscella* as marking the appearance of SBZ5. The Zhongba assemblages include *Assilina dandotica, Ass. Laminosa, Ass. granulosa, Ranikothalia nuttalli* (Plate 1, Figs 14-15), *Discocyclina* sp. A (Plate 1, Figs 16-19), *D. ranikotensis, D. sella*, *Nummulites deserti, N. mamillatus Miscellanea miscella*, and *Operculina canalifera*. TP4 is defined in the Zhongba area by the biostratigraphic ranges of *Ass. dandotica* (Plate 2, Fig. 12; see Hu et al., 2013). The top of TP4 marks also the disappearance of *Miscellanea* spp. in all areas. The TP4 assemblages of the Zongpu and the Zhepure Shan formations were deposited in a reefal environment, while those of the Jalazi and Dajin formations were deposited in forereef environment.

Biozone TP5: (Earliest Ypresian, P5b, 56.0-54.9 Ma, upper SBZ6, based on *Orbitolites complanatus*, *A. pasticillata, A. ellipsoidalis, A. aramea*) was studied from Zongpubei section (text-fig. 5), Shenkeza

section (text-fig. 8) and Dajin sections. Assemblages include *Lockhartia haimei, L. conditi, Glomalveolina subtilis, Alveolina aramaea, A. pasticillata, A. ellipsoidalis, Opertorbitolites* sp. and *Orbitolites complanatus.* TP5 in the Indian Plate is defined by the first occurrence of *O. complanatus* (Plate 1, Fig.13, 14B) and the last occurrence of *A. aramaea* or the lowest occurrence of *Alveolina nuttalli.* In the Zhongba area the assemblages are dominated by *Nummulites minervensis, Alveolina pasticillata, Assilina laminosa, Ass. granulosa, Nummulites mamillatus* (Plate 2, Fig. 6B), and *Discocyclina ranikotensis.* TP5 in the zhongba area, is defined by the first appearance of *A. pasticillata* and the stratigraphic range of *N. minervensis.* The TP5 assemblages of the Zongpu and Zhepure Shan formations in the Tingri area were deposited in a backreef to shallow reefal environment, while those of the Dajin Formation in the Zongba area were deposited in a shallow reefal to forereef environment (see text-figs 15, 17).

Biozone TP6: (lower Ypresian, P6, 54.9-52.3 Ma, Indian Plate: Zongpubei section (text-fig. 5) in Gamba area, Shenkeza (text-fig. 8), Naiqiong (text-fig. 10) and Longjiang (text-fig. 11) sections in Tingri area; Asian Plate: Dajiweng (text-fig. 14) section in the Gar area. In the Indian Plate, TP6 corresponds to the Zongpu and Zhepure Shan formations in Tingri and Gamba areas (see text-fig. 7). The lower boundary of TP6 is defined by the first occurrence of *Alveolina moussoulensis*, while the lowest occurrence of *Alveolina schwageri* serve to define the upper boundary of this zone. The assemblages in the Indian Plate are dominated mainly by *Alveolina* spp., and were deposited in a back-reef environment, while assemblages in the Asian Plate were mainly dominated by *Nummulites* and *Discocyclina* and were deposited in a shallow reefal environment. TP6 is divided into 3 subzones TP6a-c which are equivalent to the lower Ypresian (P6, see BouDagher-Fadel, 2013a,b, or SBZSBZ7-ZBZ9):

- Subzone TP6a (lowerYpresian, P6a, 54.9-54.0 Ma, corresponds to SBZ7, based on the presence of *Alveolina moussoulensis, A. regularis, A. globosa, A. nuttalli* and *Orbitolites complanatus*) was studied from Zongpubei (text-fig. 5), Shenkeza (text-fig. 8) and Longjiang (text-fig. 11) sections. The assemblages include *Alveolina moussoulensis, A. regularis, A. globosa, A. nuttalli* (Plate 2, Fig. 6A), *A. subpyrenaica, Gomalveolina subtilis* and *Orbitolites complanatus.* This

subzone is defined by the first occurrence of *A. moussoulensis* (Plate 2, Fig. 17) and the lowest occurrence of *Alveolina corbarica*.

- Subzone TP6b (lower Ypresian, early part of P6b, 54.0-53.0 Ma, corresponds to SBZ8 based on the presence of *Alveolina corbarica* and *Nummulites atacicus*) was studied from Zongpubei (text-fig. 5), Shenkeza section (text-fig. 8), Longjiang (text-fig. 11) and Dajiweng section (text-fig. 14). The assemblages in the Gamba and Tingri area include *Alveolina corbarica, A. elliptica, A. subpyrenaica, A. globose, Orbitolites gracilis, O. complanatus, Opertorbitolites lehmanni, Assilina granulosa, Ass. Laminosa, Nummulites atacicus*. In the Dajiweng section, the assemblages include *Alveolina corbarica, Nummulites globulus, N. atacicus, Alveolina globosa* (Plate 2, Fig. 21), *A. aragonensis, A. moussoulensis, A. agerensis, Assilina granulosa, Ass. laminosa, Discocyclina ranikotensis, Discocyclina sella,* and *Orbitolites megasphericus*. The biostratigraphic range of *A. corbarica* defines this subzone.
- Subzone TP6c (lower Ypresian, upper part of P6b, 53-52.3 Ma, corresponds to SBZ9 based on the presence of *Alveolina trempina*) was studied from the Zongpubei (text-fig. 5), Shenkeza (text-fig. 8), Qumiba (text-fig. 9), Naiqiong (text-fig. 10), Longjiang (text-fig. 11) and Dajiweng (text-fig. 14) sections. The assemblages include *Alveolina trempina, A. globosa, A. elliptica, A. aragonensis, A. nuttalli, A. subpyrenaica, Nummulites globulus*, *Assilina granulosa* and *Orbitolites complanatus*. This biozone is defined by the stratigraphic range of *A. trempina* (Plate 1, Fig. 24). In the absence of *A. trempina*, the upper boundary of TP6c is also defined by the lowest appearance of *Alveolina schwageri*.

Biozone TP7: (Ypresian, P7-P9a, 52.3-49.0 Ma, Indian Plate: Zongpubei section (text-fig. 5) in Gamba area, Shenkeza (text-fig. 8), Naiqiong (text-fig. 10) and Longjiang (text-fig. 11) sections in Tingri area; Asian Plate: Dajiweng (text-fig. 14) section in the Gar area. TP7 corresponds to the upper part of the Zongpu and Zhepure Shan formations in the Tingri and Gamba areas, and the Dajiweng Formation in the Gar area (see text-fig. 15). These limestones have been sampled as part of this study, and are found to be transgressional from shallow reefal to forereef facies, which are used to define Biozone 7. The lower boundary of this biozones is defined by the first occurrence of *Alveolina schwageri* and the upper boundary is defined by the disappearance of *Nummulites cantabricus* or the lowest occurrence of

Nummulites fossulata. TP7 can be divided into 2 subzones TP7a-b which are equivalent to the Ypresian, P7-P9a see BouDagher-Fadel, 2013a,b, or SBZ10 to SBZ11:

- Subzone TP7a (P7, 52.3-51 Ma, corresponds to SBZ10 based on the presence of *Alveolina schwageri, A. elliptica, Nummulites burdigalensis, Orbitolites complanatus*) was studied from Zongpubei (text-fig. 5) Shenkeza (text-fig. 8), Naiqiong (text-fig. 10), Longjiang (text-fig. 11) and Dajiweng (text-fig. 14) sections. The assemblages are dominated by reefal assemblages of *Nummulites burdigalensis, N. globulus, Alveolina schwageri, A. oblonga, A. nuttalli, A. globosa, A. elliptica, Assilina leymeriei, Orbitolites complanatus, Assilina laminosa* and *Ass. placentula.* TP7a is defined by the full biostratigraphic range of *Alveolina schwageri* (Plate 2, Fig. 14A) and *Nummulites burdigalensis* (Plate 1, Fig. 23).
- TP7b (P8-P9a, 51-49 Ma, corresponds to SBZ11, based on the presence of *Assilina placentula* and *Nummulites cantabricus*) was studied from Zongpubei (text-fig. 5), Shenkeza (text-fig. 8) and Longjiang (text-fig. 11). The assemblages are dominated by a forereef assemblage of *Alveolina nuttalli, Assilina laminosa, Ass. exponens Ass. granulosa, Ass. leymeriei, Ass. placentula, Discocyclina sella, D. dispansa, D. ranikotensis, Nummulites mamillatus* and *Nummulites cantabricus*. TP7b is defined by the full biostratigraphic range of *N. cantabricus* (Plate 2, Fig. 6c).

Biozone TP8 (P9b, 49-47.8 Ma, SBZ12, based on *Nummulites manfredi, Assilina plana* and *Nummulites fossulata*) was studied from Shenkeza (text-fig. 8), Qumiba (text-fig. 9), and Longjiang (text-fig. 11) sections. TP8 corresponds to the top-most of the Zongpu and Zhepure Shan formations in the Tingri area (the Zhepure Shanpo Formation from Willems et al., 1996). The assemblages are of a forereef setting and are dominated by *Nummulites manfredi, Assilina plana, Ass. laminosa, Ass. cuvillieri, Ass. sublaminosa* (Plate 2, Figs 18, 19A), *Ass. papillata, Nummulites fossulata, Discocyclina sella,* and *D. dispansa* (Plate 2, Fig. 19C). Planktonic foraminifera (e.g. *Subbotina eocaenica*, Plate 1, Fig. 21) are also present. TP8 is defined by the stratigraphic range of *N. manfredi* and *N. fossulata* (Plate 2, Fig. 16).

Biozone TP9 (P10-P11, 47.8-42.3 Ma, based on *Turborotalia possagnoensis, Turborotalia frontosa* and *T. pomeroli/centralis*) was studied from Zongpubei (text-fig. 5), Qumiba (text-fig. 9), Naiqiong (text-fig. 10) and Longjiang (text-fig. 11). TP9 corresponds to SBZ13-SBZ14 and represent the Enba Formation in the Indian Plate. These limestones have been sampled as part of this study, and are found to be of deep outer neritic environment. Foraminifera were mainly a mixture of reworked Cretaceous, e.g. *Globotruncana arca* and Paleogene planktonic foraminifera, e.g. *Morozovella aragonensis* (Plate 2, Fig.15A), *Subbotina eocaenica* (Plate 1, Fig. 21) but the youngest planktonic foraminifera are *Turborotalia possagnoensis*, at the bottom of the Enba Formation and *Turborotalia frontosa*, *T. pomeroli/centralis* (Plate 2, Fig. 15B) and *Morozovella lehneri* towards the top (Hu et al., submitted). This zone is defined by the first occurrence of *T. possagnoensis* and last occurrence of *T. frontosa.*

Following the definition of these biozones, we can define the biostratigraphic ages of the Late Cretaceous-Eocene marine stratigraphic units found in the Tethyan Himalaya and Xigaze basin (see Figs 2 and 3). Thus the formations from the former are the:

- Jiubao Formation is of Coniacian-Santonian in age, TLK2 (a-c) biozone. It was deposited in an inner to outer neritic environment in the Tingri and Gamba areas of the Tethyan Himalaya.
- Zongshan /Zhepure Shan Formation is of Campanian - Maastrichtian (1-2) age, TLK2 (d)-TLK3 biozones. This formation was initially deposited in an inner neritic environment in the Tingri and Gamba areas. Rapid shallowing occured towards the top of this formation corresponding to an inner/forereef environment.
- Jidula Formation is of early to middle Paleocene (Danian-Selandian, P1-Early P4) age, TP1 biozone. The limestones within the Jidula, where the foraminifera described are found, were deposited in a backreef to shallow reefal environment.
- Zongpu Formation is of late Paleocene – early Eocene (Thanetian - Ypresian, late P4-P9) age, TP2-TP8 biozones. It was deposited in a shallow reefal environment in the Tingri and Gamba areas.
- Enba Formation is of middle Eocene (early Lutetian age, P10-P11), TP9 biozone. It was deposited in an inner neritic environment in the Tingri and Gamba areas.

In the Xigaze basin (see text-fig. 15), the:

- Qubeiya Formation is of Late Maastrichtian age (Maastrichtian 3), TLK3 biozone. It is equivalent to the upper part of the Zhepure Shanpo Formation in the Tethyan Himalaya. It was deposited in a forereef environment in the Cuojiangding Zhongba area.
- Quxia Formation is of Paleocene age (late Selandian, early P4), TP1c biozone. It was deposited in a backreef environment.
- Jialazi Formation is of Thanetian age (late P4-early P5), TP2-TP4 biozones, and it was deposited in a reefal to forereefal environment.
- Dajin Formation is of early Eocene age (early Ypresian, late P5), TP5 biozone. It was deposited in a forereef environment.
- Dajiweng Formation is of early Eocene age (Ypresian, P6-P7), TP6-TP7a. This formation was deposited in a forereefal to reefal environment.

Finally, during the course of this study, we have had cause to redefine the accepted ranges of some LBF. The first appearance of many species that defined the SBZ of the Mediterranean seemed to be in need of revision in the Tethyan Himalaya. For example, *Miscellanea yvettae*, which defines the beginning of SBZ3, P4a (see BouDagher-Fadel 2013b) in the Mediterranean, appears in the Tethyan Himalaya a million years later, in late SBZ3, P4b, TP2 biozone. *Nummulites heberti* first appeared at the beginning of SBZ3, TP2 in Western Tethys, however, in the Xigaze forearc basin it does not appear until SBZ4, TP3, approximately 3 million of years later. *Assilina leymeriei* which first appear in the Western Tethys in SBZ8, does not appear in the Tethyan Himalaya before SBZ10, where it ranges from SBZ10-SBZ11, TP7a-TP7b. *Alveolina ellipsoidalis*, *A. pasticillata* and *Nummulites minervensis* appear in early SBZ6, P5a (see BouDagher-Fadel 2013b) in the Western Tethys, but they do not appear before latest SBZ6, P5b, TP5 biozone, in the Tethyan Himalaya and the Xigaze Forearc basin (see Fig 5). This later appearance of these phylogenetically root-forms in the Eastern Tethys, is compatible with the previously observed gradual eastward migration of LBF forms through the Tethyan corridor, within a few million years of their first appearance in Western Tethys (see BouDagher-Fadel and Price 2010; 2013; 2014).

Recently, Zhang, Willems and Ding (2013) argued, on the basis of species diversity, that the Eastern Tethyan LBF forms evolved and developed prior to forms in Western Tethys. They largely based this argument on secondary data presented by Scheibner and Speijer (2008) on the paleontology and biostratigraphy of the Paleocene. Our recent work on newly available field and core material (BouDagher-Fadel and Price 2010; 2013; 2014), however, enabled a global comparison to be made of Paleocene (and younger) low-latitude LBF facies, with co-occurring cosmopolitan planktonic foraminiferal forms. As noted above, we showed that the phylogenetically root-forms of LBF developed first in the west and subsequently migrated to the east, where they radiated and became diverse. These published observations, therefore, show that the hypothesis of Zhang, Willems and Ding (2013) is incompatible with planktonic foraminiferal biostratigraphic correlation.

PALEOENVIRONMENT OF THE CARBONATE FACIES IN SOUTHERN TIBET

Diverse assemblages of PF in the neritic facies, and of LBF and algae in the reefal platforms have contributed to the facies development of the southern Tibetan carbonates. These microfaunas and microfloras are sensitive to changes of water depths and climate, and as is in keeping with the paleoogeographic reconstructions, the constant presence of LBF throughout the Paleocene and early Eocene suggests a warm equatorial climate during this period.

A depositional model has been postulated for the Late Cretaceous-Eocene carbonate facies in the both sides of the eastern Tethyan Ocean and is summarised in text-fig. 17. The Gamba and Tingri sections were deposited on the northern margin of the Indian Plate, while the Cuojiangding, Dajin and Dajiweng sections were laid down on the southern margins of the Asian Plate. In the Late Cretaceous, the matrix and the organic components of the samples are divided into two parts on both sides of the Yarlung Zangbo suture, an older part of Late Cretaceous age with a mitiric matrix and a younger latest Cretaceous part that included fragments of algae, calcareous hyaline larger benthic foraminifera planktonic foraminifera assemblages all cemented by sparite. A deep outer neritic environment prevailed in the

Coniacian to early Maastrichtian, where TLK2 assemblages of the Jiubao Formation and the lower part of Zongshan Formation were dominated by strongly keeled planktonic foraminifera (BouDagher-Fadel, 2013a). However, in the late Maastrichtian the warm climate was accompanied by a sudden global sea-level drop as observed in the northern Indian margin interpreted as a tectonic uplift related to the Deccan doming (see text-fig. 1; Garzanti and Hu 2014), where TLK2 assemblages were replaced abruptly by LBF TLK3 assemblages of the Zongshan and Zhepure Shanpo formations. The LBF assemblages of the TLK3 favoured forereef environments, and are found with small fragments of rhodophyte algae. It is generally accepted that orbitoids found in TLK3 thrived in shallow tropical and subtropical seas, in areas with little or no clastic influx (van Gorsel 1975) and were sustained by symbiotic species (BouDagher-Fadel 2008). The extinction of the orbitoids at the end of the Maastrichtian coincided with a global extinction of many other larger benthic foraminifera (BouDagher-Fadel, 2008), and indeed other forms.

The early Paleocene was a period of post, mass-extinction recovery, and the Danian and Selandian mark the start of the global recovery period for both LBF and PF (BouDagher-Fadel 2008; 2013a). During this period, on the northern margin of the Indian Plate, intermittently occurring TP1 assemblages established themselves in a back reef to open-marine, shallow reefal setting, where small miliolids and rotaliids dominated the occasional limestone assemblages of the Jidula Formation.

By the Thanetian TP2 and TP3 assemblages were thriving in a shallow reefal environment on the northern margin of the Indian Plate and in the southern margin of the Asian Plate. However, assemblages occurring on the margins of the Indian Plate were more diverse than those of the Asian Plate, and included small orbitoids such as *Orbitosiphon* (Plate 2, Fig. 10).

By end of the Paleocene, the Earth's climate went through the warmest period of the entire Cenozoic, which included the Paleocene-Eocene Thermal Maximum (PETM). From early to middle Eocene, the average global sea-water temperatures rose by 6ºC (Macleod, 2013). During the early to earliest middle Eocene, different assemblages of LBF were established. In the earliest Eocene (early Ypresian) TP5 – TP7, miliolids and alveolinids (*Alveolina*) became important components of the assemblages in the

Zongpu Formation on the northern margin of the Indian Plate and the Dajiweng Formation on the southern margin of the Asian Plate. Their constant presence throughout the early Eocene suggests an eutrophic and well oxygenated environment with warm, clear and calm waters, locally low inputs of clastic sediments, and affected by waves. In the Middle Ypresian, sea-levels rose to a record high stand around 53 Ma (see Miller et al. 2005), and the reefal *Alveolina* species became rare and were completely replaced by *Nummulites* and *Discocyclina* in the TP8 of the Zongpu Formation on the northern margin of the Indian Plate. *Nummulites* thrived in the warm tropical waters in the Ypresian on both sides of the eastern Tethyan Ocean, but rapidly disappeared at the onset of the middle Eocene (Lutetian), when the sea level changed abruptly. In the early Lutetian, high sea-levels coupled with humid climate, and inferred incipient tectonic processes induced enhanced rates of continental erosion, increased runoff and high clastic input into the carbonates facies, which consequently overwhelmed and inhibited the pre-existing carbonate-dominated depositional conditions. In general, TP9 assemblages of the Enba Formation are of an inner neritic environment. Larger benthic reefal assemblages disappear completely, except for rare reworked forms, and the sediments are composed of a mixture of Cretaceous, Paleocene, early Eocene reworked material and in situ earliest Middle Eocene (Lutetian) planktonic foraminifera.

CONCLUSION

Planktonic foraminifera and LBF dominate the Late Cretaceous-early Paleogene carbonates of the northern margin of the Indian Plate and of the southern margin of the Asian Plate. The PF thrived in the inner to outer, neritic environment and their well-defined biostratigraphic ranges enables them to be used in global correlation. On the other hand, LBF thrived on reefal platforms and were the main components of the latest Cretaceous to early Eocene assemblages. During this time, adaptive radiations in the LBF and environmental control of growth-forms make them reliable regional biostratigraphic and paleoenvironmental indicators.

We found that the Late Cretaceous-early Paleogene carbonate successions in the Tibetan Himalayas evolved during six depositional stages, which we divided into 11 biozones (TLK2-3 and TP1-9). The

first stage occurred in the Late Cretaceous, where deep outer to inner neritic waters prevailed; keeled planktonic foraminifera were the main components of the assemblages (TLK2), which were replaced in the latest Maastrichtian by forereef assemblages dominated by of *Lepidorbitoides, Omphalocyclus* and *Orbitoides* species (TLK3). Following the end Cretaceous global extinction, the Paleocene saw shallow reefal environments become re-established during an increasingly global warm period. Temperature-sensitive organisms, such as LBF, thrived during this period, with benthic assemblages dominated by small miliolids and rotaliids such as *Ranikothalia, Daviesina* and *Lockhartia* (TP1-2). In the late Paleocene – early Eocene, the shallow reefal environment was dominated by warm water forms such as *Alveolina, Assilina* and *Nummulites* (TP3-7). At the end of the early Eocene, the depositional environment is characterised by a slight deepening of the water, following the rise in global sea level, during which forereef assemblages dominated by LBF such as *Nummulites* and *Discocyclina* (TP8) were established. Finally the final depositional stage (TP9) reflects a rapid disappearance of the reefal shallow carbonate waters at the onset of the Middle Eocene, coeval with and probably induced by the onset of the tectonic movements leading to the collision of the Indian and Asian Plates. This resulted in the replacement of the reefal LBF by pelagic sediments containing PF. Tectonic movements resulted in reworking of many assemblages, such as the Cretaceous *Globortruncana* and the Paleocene and Eocene *Morozovella* within the early Lutetian assemblages including *Turborotalia* spp.

The presence of PF specimens at some levels (e.g., see Plate 1 Figs 20-21; Plate 2, Fig. 15), and their co-occurrence with LBF forms, has provided a rare opportunity to correlate the biostratigraphic framework of these two groups. We have confirmed our earlier observations that some LBF forms appear about 1-3 million years later in the eastern part of Tethys than they do in the west, reflecting the previously inferred gradual eastern paleogeographic migration of these forms. This resulting new correlation of Eastern and Western Tethyan LBF biozones is of global stratigraphic importance, as it allows us to produce for the first time a pan-Tethyan LBF biozonation scheme.

APPENDIX: COMMENTS ON UNNAMED TAXA

The two species, *Lepidorbitoides* sp. A and *Discocyclina* sp. A, are placed here in open nomenclature, as the specimens obtained are from random thin sections of limestones. Biometric measurements on isolated, solid specimens of larger foraminifera have rarely been possible, we therefore attempt to describe them by combining the broad results gained from equatorial sections of the megalospheric nepiont of the orbitoids (as published by Drooger 1993) with those obtained by vertical sections of the whole test (as followed by BouDagher-Fadel 2008). We use as well the broad results gained by equatorial sections of the megalospheric nepiont of the discocyclinds (as published by Özcan et al. 2007), with those obtained from vertical sections of the whole test (see BouDagher-Fadel 2008).

Class FORAMINIFERA Lee 1990

Family Lepidorbitoididae Vaughan 1933

Genus *Lepidorbitoides* Silvestri 1907

Type species*: Orbitoides socialis* Leymerie 1851

Lepidorbitoides sp. A

Plate 1, Figs 1-8

Type locality: Tibet, Xigaze forearc basin, Zhongba, County, the Cuojiangding section (09CJD25-09QX-B02), 11 km 40 degrees NE of the Qiongguo Village (Hu et al., submitted).

Number of specimens embedded in the studied samples: 48 specimens

Dimensions: Maximum measured longest diameter (MMLD) 10mm.

Description: The test is lenticular with a slightly raised centre and is slowly tapering towards the margins. Thickness of the central part of the test is 1mm to 1.2mm in megalospheric forms (Plate 1, Figs 1-3, 8), but only 0.6mm to 0.7mm in microspheric forms (Plate 1, Figs 5-7). Ratio of diameter to thickness 4:1 in megalospheric forms, 7:1 in microspheric forms. The bilocular embryo comprises a circular protoconch and a slightly reniform deuteroconch, both almost equal in size (see Plate 1, Figs 1, 8). The deuteroconch forms 43% of the embryonic apparatus. The equatorial chambers are spatulate to

becoming irregularly hexagonal in shape. About 6 to 7 layers of lateral chamberlets with thin walls are regularly stacked on either side of the equatorial layer. They are thin-walled with uniform shape; their size decreases gradually from the centre to periphery of test. As noticed in thin sections, the height of lateral chamberlets is approximately 53µm near the centre to 47 µm near the periphery, while the height of equatorial chamberlets ranges from 70 µm to 80µm. The last 4 to 5 rows of chambers are with pillars, which become very concentrated, forming pustules, near the periphery of the test.

Remarks: The shape of the test and concentrated pillars near the periphery distinguish this species from *Lepidorbitoides blanfordi* Rao, and the size of the tests, the slightly raised centre and the concentrated pustules near the periphery distinguishes this species from *Lepidorbitoides minor* (Schlumberger).

Distribution: late Maastrichtian (LK3), Xigaze forearc basin, Cuojiangding Zhongba, Tibet.

Family Discocyclinidae Galloway 1928

Genus *Discocyclina* Guembel 1870

Type species: *Orbitolites prattii* Michelin 1846

Discocyclina sp. A

Plate 1, Figs 16-19

Type locality: Tibet, Xigaze forearc basin, Zhongba County, the Cuojiangding section, 09QX-B33-09JLZ06B, 11 km 40 degrees NE of Qiongguo Village (Hu et al., submitted).

Number of specimens embedded in the studied samples: 32 specimens

Dimensions: Maximum measured longest diameter (MMLD) 5mm.

Description: A *Discocyclina* with a lenticular, flat test. The embryonic apparatus is large, making up 14% of the test. The measured outer diameter of the protoconch is approximately double that of the deuteroconch when measured perpendicular to their common axis. The equatorial layer is composed of concentric rings of elongated narrow rectangular chamberlets (8 times longer than narrower) with a curved base, those of successive cycles alternating in position. Lateral chamberlets are of irregular size and are irregularly stacked. Pillars are absent.

Remarks: This species differs from *Discocyclina ranikotensis* in having a lenticular instead of a discoidal test, and by the irregularity in size and shape of the lateral chamberlets. Fine, short pillars

between the chamberlets may be found in the centre of the microspheric forms (see Plate 1, Fig. 19B) but radiating only from the 6th row of lateral chamberlets.

Distribution: This species is found in Tibet, Xigaze forearc basin, Cuojiangding Zhongba, late Paleocene, SBZ5, TP4, Tibet.

ACKNOWLEDGEMENTS

We would like to thank Prof. Christopher R. Scotese for his permission to use his paleoogeographic map as illustration in our article. We acknowledge input from the reviewers and especially thank Prof. Johannes Pignatti for his constructive comments. We are also grateful to Dr. Lucy E. Edwards for reviewing our paper and for her valuable comments. We thank Wei An, Hehe Jiang, Juan Li, Gaoyuan Sun, Jiangang Wang, and Cong Wu for their help in sampling in the field. This study was financially supported by the Strategic Priority Research Program (B) of the Chinese Academy of Sciences (XDB03010100), the Chinese MOST 973 Project (2012CB822001), and the NSFC Project (41172092).

REFERENCES

ADAMS, C.G., 1984. Neogene larger foraminifera, evolutionary and geological events in the context of datum planes. In: Ikebe, I., Tsuchi, R. (Eds), *Pacific Neogene Datum Planes.* University of Tokyo Press, Tokyo: 47–68.

AFZAL, J., WILLIAMS, M., LENG, M.J., ALDRIDGE, R.J. and STEPHENSON, M.H., 2011. Evolution of Paleocene to Early Eocene larger benthic foraminifer assemblages of the Indus Basin, Pakistan. *Lethaia*, 44: 299–320.

AN, W., HU, X., GARZANTI, E., BOUDAGHER-FADEL, M., WANG, J. and SUN, G., 2014. The Xigaze Forearc Basin revisited: provenance changes and origin of the Xigaze Ophiolite. *Geological Society of America Bulletin*, 126(11-12): 1595-1613.

BERGGREN, W.A., 1973. The Pliocene time scale: calibration of planktonic foraminiferal and calcareous nannoplankton zones. *Nature*, 243: 391–397.

BLOW, W.H., 1979. The Cainozoic Globigerinida: A Study of the Morphology, Taxonomy, Evolutionary Relationships and the Stratigraphical Distribution of Some Globigerinida, 3. Brill, Leiden.

BOUDAGHER-FADEL, M.K., 2008. *Evolution and Geological Significance of Larger Benthic Foraminifera*. Developments in Palaeontology and Stratigraphy, 21, 540p.

BOUDAGHER-FADEL, M.K., 2013a. *Biostratigraphic and Geological Significance of Planktonic Foraminifera,* 2nd edition. OVPR UCL, London, http://dx.doi.org/10.14324/99.1, 307p.

BOUDAGHER-FADEL, M.K., 2013b. Diagnostic First and Last Occurrences of Mesozoic and Cenozoic Planktonic Foraminifera,.OVPR UCL, London, *Professional Papers Series*, 1: 1-4.

BOUDAGHER-FADEL, M.K. and BANNER, F.T., 1999. Revision of the stratigraphic significance of the Oligocene–Miocene 'letter-Stages'. *Revue de Micropaléontologie*, 42: 93–97.

BOUDAGHER-FADEL, M.K. and PRICE, G.D., 2010. The evolution and palaeogeographic distribution of the Lepidocyclinids. *Journal of Foraminiferal Research,* 40: 81–110.

BOUDAGHER-FADEL, MK and PRICE, G.D., 2013. The phylogenetic and palaeogeographic evolution of the miogypsinid larger benthic foraminifera. *Journal of the Geological Society,* 170: 185 - 208.

BOUDAGHER-FADEL, M.K. and PRICE, G.D., 2014. The phylogenetic and palaeogeographic evolution of the nummulitoid larger benthic foraminifera. *Micropaleontology,* 60, 5,: 483-508.

CHAPRONIÈRE, G.C.H., 1984. The Neogene larger foraminiferal sequence in the Australian and New Zealand regions, and its relevance to the East Indies letter stage classification. *Palaeogeography, Palaeoclimatology, Palaeoecology*, 46: 25–35.

DING, L., KAPP, P. and WAN, X.Q., 2005. Paleocene-Eocene record of ophiolite obduction and initial India-Asia collision, south central Tibet. *Tectonics,* 24, doi:10.1029/2004TC001729.

DROOGER, C.W., 1993. Radial foraminifera, morphometrics and evolution. *Verhandelingen der Koninklijke Nederlandse Akademie van Wetenschappen, Afd. Natuurkunde, Erste Reeks*, Amsterdam, deel 41, 241p.

DÜRR, S.B., 1996. Provenance of Xigaze fore-arc basin clastic rocks (Cretaceous, south Tibet). *Geological Society of America Bulletin*, 108: 669-684.

EINSELE, G., LIU, B., DÜRR, S., FRISCH, W., LIU, G., LUTERBACHER, H.P., RATSCHBACHER, L., RICKEN, W., WENDT, J., WETZEL, A., YU, G. and ZHENG, H., 1994. The Xigaze forearc basin: evolution and facies architecture (Cretaceous, Tibet). *Sedimentary Geology*, 90: 1-32.

GANSSER, A., 1964. *Geology of the Himalayas*. Interscience Publishers John Wiley and Sons, London.

GANSSER, A., 1980. The significance of the Himalayan suture zone. *Tectonophysics*, 62: 37-52.

GARZANTI, E. and HU, X., 2014, Latest Cretaceous Himalayan tectonics: Obduction, collison or Deccan-related uplift? *Gondwana Research*, ttp://dx.doi.org/10.1016/j.gr.2014.03.010.

GRADSTEIN, F.M., OGG, J.G., SCHMITZ, M.D. and OGG, G.M. 2012. *The Geologic Time Scale 2012*, Elsevier, 2 volumes: 1144 p.

HE, Y., ZHANG, B.G., HU, LY. and SHEN, J.Z., 1976. *The report of the Scientific Expedition in the Jolmo Lungma Region.* Beijing Science Press, 76p.

HU, X., JANSA, L., CHEN, L., GRIFFIN, W.L., O'REILLY, S.Y. and WANG, J., 2010. Provenance of Lower Cretaceous W long Volcaniclastics in the Tibetan Tethyan Himalaya: Implications for the final breakup of Eastern Gondwana. Sedimentary *Geology*, 223: 193-205.

HU, X., SINCLAIR, H. D., WANG, J., JIANG, H. and WU, F., 2012. Late Cretaceous-Paleogene stratigraphic and basin evolution in the Zhepure Mountain of southern Tibet: implications for the timing of India-Asia initial collision. *Basin Research*, 24: 520-543.

HU, X, WANG, J., BOUDAGHER-FADEL, M., GARZANTI, E. and WEI, A., 2013. Transition From Forearc Basin to Syn-Collisional Basin in Southern Tibet (Paleocene Cuojiangding Group): Implication to Timing of the India-Asia Initial Collision and of Yarlung Zangbo Ophiolite Emplacement, *Acta Geologica Sinica*, 87: 27-28.

JADOUL, F., BERRA, F. and GARZANTI, E., 1998. The Tethyan Himalayan passive margin from late Triassic to early Cretaceous (South Tibet). *Journal of Asian Earth Sciences*, 16: 173-194.

JAUHRI, A. K. and AGARWAL, K. K., 2001. Early Paleogene in the south Shillong Plateau, NE India: local biostratigraphic signals of global tectonic and oceanic changes. *Palaeogeography, Palaeoclimatology, Palaeoecology*, 168: 187-203.

LI, J., HU, X.M., GARZANTI, E., AN, W. and WANG, J.G., 2014. Paleogene carbonate microfacies and sandstone provenance (Gamba area, South Tibet): Stratigraphic response to initial India–Asia continental collision. *Journal of Asian Earth Sciences*, doi.org/10.1016/j.jseaes.2014.10.027.

MILLER, K.G., KOMINZ, M.A., BROWNING, J.V., WRIGHT, J.D., MOUNTAIN, G.S., KATZ, M.E., SUGARMAN, P.J., CRAMER, B.S., CHRISTIE-BLICK, N. and PEKAR S.F., 2005. The Phanerozoic Record of Global Sea-Level Change. *Science*, 310, 1293, DOI: 10.1126/science.1116412.

MACLEOD, N. 2013 *The Great Extinctions: What Causes Them and How They Shape Life*. Natural History Museum, London: 208p.

NAJMAN, Y., APPEL, E., BOUDAGHER-FADEL, M., BOWN, P., CARTER, A., GARZANTI, E., GODIN, L., HAN, J.T., LIEBKE, U., OLIVER, G., PARRISH, R. and VEZZOLI, G., 2010. Timing of India–Asia collision: geological, biostratigraphic, and palaeomagnetic constraints. *Journal of Geophysics Research*, 115, B12416, doi:10.1029/2010JB007673.

ÖZCAN, E., LESS, G.Y., BÁLDI-BEKE, M., KOLLÁNYI, K. and KERTÉSZ, B. 2006. Biometric analysis of middle and upper Eocene Discocyclinidae and Orbitoclypeidae (Foraminifera) from Turkey and updated orthophragmine zonation in the Western Tethys. *Micropaleontology*, 52: 485-520

PATZELT, A., WANG, H. LI, J. and APPEL, E. 1996. Palaeomagnetism of Cretaceous to Tertiary sediments from southern Tibet: Evidence for the extent of the northern margin of India prior to the collision with Eurasia. *Tectonophysics*: 259, 259–284, doi:10.1016/0040-1951(95)00181-6

RACEY, A., 1995. Lithostratigraphy and Larger Foraminiferal (Nummulitid) Biostratigraphy of the Tertiary of Northern Oman. *Micropaleontology Supplement*: 41: 1-123.

RATSCHBACHER, L., FRISCH, W., LIU, G. and CHEN, C.C., 1994. Distributed deformation in southern and western Tibet during and after the India–Asian collision. *Journal of Geophysical Research*, 99, 19,917–19,945, doi:10.1029/94JB00932.

SERRA-KIEL, J., HOTTINGER, L., CAUS, E., DROBNE, K., FERRANDEZ, C., JAUHRI, A.K., LESS, G., PAVLOVEC, R., PIGNATTI, J., SAMSO, J.M., SCHAUB, H., SIREL, E., STROUGO, A., TAMBAREAU, Y., TOSQUELLA, J. and ZAKREVSKAYA, E., 1998. Larger foraminiferal

biostratigraphy of the Tethyan Paleocene and Eocene. *Bulletin de la Société géologique de France*, 169: 281–299.

SCHEIBNER, C. and SPEIJER, R. P, 2008. Decline of coral reefs during late Paleocene to early Eocene global warming, *eEarth*, 3: 19–26, www.electronic-earth.net/3/19/2008/.

VAN GORSEL, J.T., 1975. Evolutionary trends and stratigraphic significance of the Late Cretaceous helicorbitoides–lepidorbitoides lineage. Utrech Micropaleontological Bulletins, 12: 1–19.

VAN DER VLERK, I.M. and UMBGROVE, J.H., 1927. Tertiary Gidsforaminifera van Nederladisch Oost-Indie. *Wetenschappelijke Mededeelingen van de Dienst van de Mijnbouw in Nederlandsch-Oost-Indie*, 6: 3–35.

WADE, B.S., PEARSON, P.N., BERGGREN, W.A. and PÄLIKE, H., 2011. Review and revision of Cenozoic tropical planktonic foraminiferal biostratigraphy and calibration to the geomagnetic polarity and astronomical time scale. *Earth-Science Reviews*, 104: 111–142.

WAN, X., 1987. Foraminifera Biostratigraphy and Paleogeography of the Tertiary in Tibet. *Geoscience*, 1: 15-47.

WAN, X., 1992. Cretaceous foraminifera from southern Xizang (Tibet): a study on eustatic change. *Geoscience*, 6: 392-398.

WAN X., JANSA, L.F. and SARTI, M., 2002. Cretaceous and Paleogene boundary strata in southern Tibet and their implication for the India–Eurasia collision. *Lethaia*, 35: 131–146. Oslo. ISSN 0024-1164.

WANG, C.S., LI, X.H., LIU, Z.H., LI, Y.L., JANSA, L., DAI, J.G. and WEI, Y.S., 2012. Revision of the Cretaceous–Paleogene stratigraphic framework, facies architecture and provenance of the Xigaze forearc basin along the Yarlung Zangbo suture zone. *Gondwana Research*, 22: 415–433.

WANG, J.-G., HU, X.-M., BOUDAGHER-FADEL, M., WU, F.-Y. and SUN, G.-Y., 2014. Early Eocene sedimentary recycling in the Kailas area, southwestern Tibet: implications for the initial India-Asia collision. *Sedimentary Geology*, 315: 1–13. doi:10.1016/j.sedgeo.2014.10.009

WENDLER, I., WENDLER, J., GR FE, K.U., LEHMANN, J. and WILLEMS, H., 2009. Turonian to Santonian carbon isotope data from the Tethys Himalaya, southern Tibet. *Cretaceous Research*, 30: 961-979.

WENDLER, I., WILLEMS, H., GRAFE, K.-U., DING, L. and LUO, H., 2011. Upper Cretaceous inter-hemispheric correlation between the Southern Tethys and the Boreal: chemo-and biostratigraphy and paleoclimatic reconstructions from a new section in the Tethys Himalaya, S-Tibet. *Newsletters on Stratigraphy,* 44: 137-171.

WILLEMS, H., ZHOU, Z., ZHANG, B. and GRÄFE, 1996. Stratigraphy of the Upper Cretaceous and lower Tertiary strata in the Tethyan Himalayas of Tibet (Tingri area, China). Geologische Rundschau, 85: 723–754, doi:10.1007/BF02440107.

WILLEMS, H., and ZHANG, B. 1993. Cretaceous and Lower Tertiary sediments of the Tibetan Himalaya in the area of Gamba (South Tibet, PR China). *Fachbereich Geowissenschaften,*,Universitat Bremen, 38:3–27.

ZHANG, Q.H., WILLEMS, H., DING, L., GRÄFE, K.U. and APPEL, E., 2012. Initial India–Asia Continental Collision and Foreland Basin Evolution in the Tethyan Himalaya of Tibet: Evidence from Stratigraphy and Paleontology. *Journal of Geology,* 120: 175–189.

ZHANG, B.G., 1988. Orbitolites from Longjiang of Tingri, Xizang (Tibet). *Acta Micropalaeontologica Sinica*, 5: 1-13.

ZHANG, Q.H., WILLEMS, H. and DING, L., 2013. Evolution of the Paleocene-Early Eocene larger benthic foraminifera in the Tethyan Himalaya of Tibet, China. *International Journal of Earth Sciences, Geologische Rundschau.* Doi: 10.1007/s00531-012-0856-2.

ZHU, D.C., ZHAO, Z.D.,NIU, Y.L., MO, X.X., CHUNG, S.L., HOU, Z.Q., WANG, L.Q. and WU, F.Y., 2011. The Lhasa Terrane: record of a microcontinent and its histories of drift and growth. *Earth and Planetary Science Letters*, 301: 241–255.

Figure captions

TEXT-FIGURE 1. Paleogeographic and tectonic reconstruction of the early Eocene (by Christopher R. Scotese). www.globalgeology.com

TEXT-FIGURE 2. Geological sketch map of the Himalayas

TEXT-FIGURE 3. Foraminiferal distribution of the Jiubao section in Gamba area in correlation to the Tibet Zones as defined by this work.

TEXT-FIGURE 4. Foraminiferal distribution of the Jidula section in Gamba area in correlation to the Tibet Zones as defined by this work.

TEXT-FIGURE 5. Foraminiferal distribution of the Zongpubei section in Gamba in correlation to the Tibet Zones as defined by this work. The dotted line shows a disconformity between Zongpu and Enba formations, where TP8 is missing. The arrow represents a thrust fault. The older Zongpu Formation thrust over the Zhaguo Formation.

TEXT-FIGURE 6. Foraminiferal distribution of the Gelamu section in Tingri in correlation to the Tibet Zones as defined by this work. The dotted line represents a disconformity at the lowest bed of Zhepure Shanpo in this section, where 2.1 Million of years of early Maastrichtian deposits (Maastrichtian 1, see BouDagher-Fadel, 2013) are eroded or missing. This is confirmed by the first occurrence of *Globotruncanita conica* and *Abathomphalus mayaroensis* confirming the presence of upper deposits of TLK2d (see BouDagher-Fadel, 2013 and text-figure 4).

TEXT-FIGURE 7. Foraminiferal distribution of the Zhepure Shanpo section in Tingri in correlation to the Tibet Zones as defined by this work.

TEXT-FIGURE 8. Foraminiferal distribution of the Shenkeza section in Tingri in correlation to the Tibet Zones as defined by this work.

TEXT-FIGURE 9. Foraminiferal distribution of the Qumiba section in Tingri in correlation to the Tibet Zones as defined by this work. The arrow represents a thrust fault. The older bed, TP2 of Zongbu is overlying the younger bed, TP7. The dotted line shows a disconformity between TP2 and TP6 in the Zongpu Formation at Qumiba.

TEXT-FIGURE 10. Foraminiferal distribution of the Naiqiong section in Tingri in correlation to the Tibet Zones as defined by this work. The arrow represents a thrust fault. The older Zongpu Formation thrust over the Zhaguo Formation.

TEXT-FIGURE 11. Foraminiferal distribution of the Longjiang section in Tingri in correlation to the Tibet Zones as defined by this work.

TEXT-FIGURE 12. Foraminiferal distribution of three sections in the Cuojiangding, Zhongba area in correlation to the Tibet Zones as defined by this work. The dotted line indicates a disconformity at the bottom of the Quxia Formation where TP1 biozone is missing.

TEXT-FIGURE 13. Foraminiferal distribution of two sections from Dajin, Burang in correlation to the Tibet Zones as defined by this work.

TEXT-FIGURE 14. Foraminiferal distribution of the Dajiweng section, Gar in correlation to the Tibet Zones as defined by this work.

TEXT-FIGURE 15. Sections studied, plotted in correlation with SBZ, Planktonic Foraminiferal Zones after BouDagher-Fadel (2013) and Tibet Zones as defined in this work. The time scale is from Gradstein et al. (2012).

TEXT-FIGURE 16. Range chart of key species in the Asian Plate and on the northern Indian Plate margin, in correlation with SBZ, Planktonic Foraminiferal Zones after BouDagher-Fadel (2013) and Tibet Zones as defined in this work. The time scale is from Gradstein et al. (2012).

TEXT-FIGURE 17. The depositional environments which prevailed during the early Eocene in the Asian Plate and on the northern Indian Plate margin.

Plate Captions

Plate 1

Figs 1-8. *Lepidorbitoides* sp. A, Late Cretaceous (3), TLK3, Cuojiangding Zhongba; 1, holotype, megalospheric form, sample 09QX-A04, x17; 2-8, paratypes, 2-4 megalospheric forms, 2, sample 09QX-A24, x 10, 3, sample 09QX-A25B, x14; 4, sample 09QX-A26, x10; 5-8, microspheric forms, 5, 8, equatorial sections, 6-7, axial sections, 5, sample 09QXA13, x8, 6-7, sample 09QX-B02, 6, x9, 7, x10, 8, sample 09QX-A25B, x20.

Figs 9. *Miscellanea yvettae* Leppig, Paleocene, SBZ 4, TP3, 11, Cuojiangding Zhongba, sample 09QX-B13, x7.

Fig. 10. *Ranikothalia sindensis* (Davies), *Miscellanea yvettae* Leppig, Paleocene, SBZ 4, TP3, Cuojiangding Zhongba, sample 09QX-B13, x8.

Fig. 11. A. *Ranikothalia thalica* (Davies), B. *Ranikothalia sindensis* (Davies), Paleocene, SBZ 4, TP3, Cuojiangding Zhongba, sample 09QX-B13, x10.

Fig. 12. *Nummulites heberti* (Muniez-Chalmas), Paleocene, SBZ 4, TP3, Cuojiangding Zhongba, sample 09JLZ05, x13.

Fig. 13. *Miscellanea yvettae* Leppig, Paleocene, SBZ 4, TP3, Cuojiangding Zhongba, sample 09QX-B13, x7.

Figs 14-15. *Ranikothalia nuttalli* (Davies), late Paleocene, SBZ5, TP4, Cuojiangding Zhongba, 14, sample 09QX-B33, x10; 15, sample 09QX-B30, x7.

Figs 16-19. *Discocyclina cuojia* new species, late Paleocene, SBZ5, TP4, Cuojiangding Zhongba: 16, holotype, 17-19, paratypes; 16-17, sample 09QX-B34B, 16, x22, 17, x8; 18, sample 09JLZ02B, x22; 19, A, megalospheric form, B, microspheric form, sample 09JLZ03B, x13.

Fig. 20. *Pseudomenardella ehrenbergi* (Bolli). Paleocene, SBZ 4, TP3, Cuojiangding Zhongba, sample 09QX-B13, x60.

Fig. 21. *Subbotina eocaenica* (Terquem). Shenkeza section, middle Eocene, TP8, sample 09SKZ-M5-18, x50.

Fig. 22. Packstone of *Assilina subspinosa* Davies, late Paleocene, TP3, Cuojiangding Zhongba, sample 09QX-B34B, x13.

Fig. 23. *Nummulites burdigalensis* cf. *kuepperi* Schaub, early Eocene, SBZ10, TP7a, Dajiweng Zhongba, 12DJW11, x10.

Fig. 24. *Alveolina trempina* Hottinger, early Eocene, SBZ9, TP6c, Dajiweng Zhongba, sample 12DJW09, x15.

Plate 2

Fig. 1. Packstone of planktonic foraminifera A: *Marginotruncana pseudolinneiana* Pessagno, Jiubao section, Santonian (2), TLK2a, sample 10GuB11vi, x20.

Fig. 2. *Concavatotruncana concavata* (Brotzen), Jiubao section, Santonian (2), TLK2, sample 10GuB11, x30.

Fig. 3. *Lepidorbitoides minor* (Schlumberger). Jidula section, Maastrichtian (3), TLK3, sample 10JDL06, x13

Figs 4. *Orbitoides medius* (d'Archiac). Jidula section, Maastrichtian (3), TLK3, 3-5, sample 10JDL05, x18.

Fig. 5. *Omphalocyclus macroporus* (Lamarck). Jidula section, Maastrichtian (3), TLK3, 7, sample 10JDL19, x15.

Fig. 6. A. *Alveolina nuttalli* Davies, B. *Nummulites mamillatus* (Fichtel & Moll), C. *Nummulites cantabricus* Schaub, Shenkeza Tingri section, Zhepure Shanpo Formation, sample 09SKZ-M5-14, TP7b, x8.

Fig. 7. *Assilina leymeriei* Archiac and Haime. Xigaze Forearc Basin, Dajiweng Zhongba, Dajieng Formation, sample 12DJW07, TP6b, x15.

Fig. 8. *Daviesina langhami* Smout. Zongpubei section, Paleocene, TP1c, Sample 10ZPB47, x16.

Fig. 9. *Lockhartia conditi* (Nuttall). Jidula section, Selandian, TP1c, sample 10JDL32, x25.

Fig. 10. *Orbitosiphon punjabensis* (Davies). Zongpubei section, Paleocene, TP2, sample 10ZPB49, x14.

Fig. 11. *Miscellanea miscella* (d'Archiac and Haime). Zongpubei section, Paleocene, TP4, sample 10ZPB34, x28.

Fig. 12. *Assilina dandotica* Davies, late Paleocene, TP4, Sample 09JLZ0, x14.

Fig. 13. *Orbitolites complanatus* Lamarck, Zongpubei section, TP7a, sample 10ZPB30, x5.

Fig. 14. A. *Alveolina schwageri* Checchia-rispoli, B: *Orbitolites complanatus* Lamarck, small miliolids, Zongpubei section, TP7a, sample 10ZPB27, x13.

Fig. 15. Packstone of planktonic foraminifera: A.: *Morozovella aragonensis* (Nuttall), B. *Turborotalia centralis* (Toumarkine and Bolli). Zongpubei section, middle Eocene, P11, TP9, sample 10ZPB16, x10.

Fig. 16. *Nummulites fossulata* de Cizancourt. Shenkeza section, middle Eocene, TP8, sample 13SKZ02, x12.

Fig. 17. *Alveolina moussoulensis* Hottinger. Qumiba section, early Eocene, TP6b, 09QMB1-1, x10.

Fig. 18. *Assilina sublaminosa* Gill. Shenkeza section, middle Eocene, TP8, sample 09SKZ-M5-14, x15.

Fig. 19. A. *Assilina sublaminosa* Gill, B. *Discocyclina sella* (Archiac), C. *Discocyclina dispansa* (Sowerby). Qumiba section, middle Eocene, TP8, sample 09QMB6-4, x10

Fig. 20. *Aberisphaera gambanica* Wan. Shenkeza section, Paleocene, TP3, 09SKZ-M4-16, x20.

Fig. 21. *Alveolina globosa* Leymerie. Qumiba section, early Eocene, TP7a, 09QMB5-3, x15.

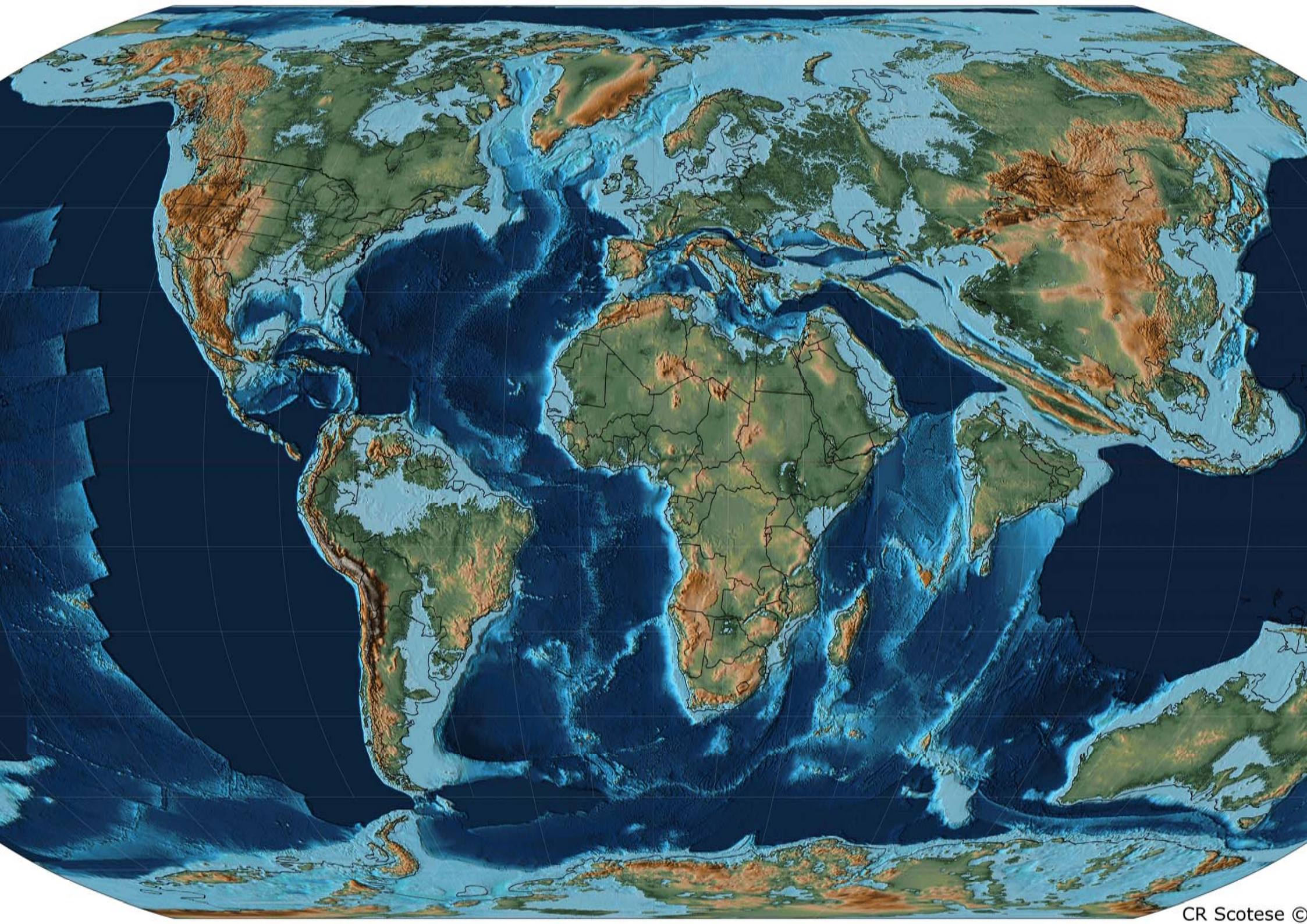
CR Scotese ©

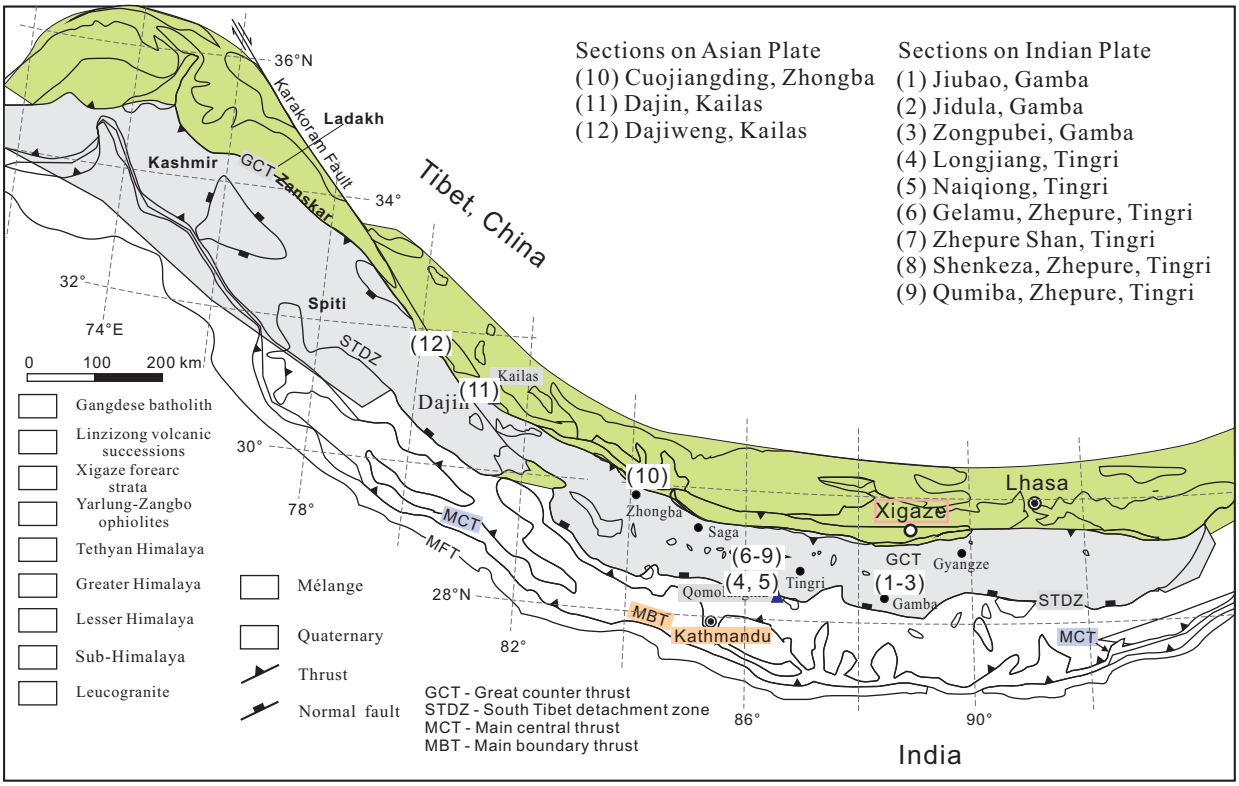
Sections on Asian Plate
(10) Cuojiangding, Zhongba
(11) Dajin, Kailas
(12) Dajiweng, Kailas
Sections on Indian Plate
(1) Jiubao, Gamba
(2) Jidula, Gamba
(3) Zongpubei, Gamba
(4) Longjiang, Tingri
(5) Naiqiong, Tingri
(6) Gelamu, Zhepure, Tingri
(7) Zhepure Shan, Tingri
(8) Shenkeza, Zhepure, Tingri
(9) Qumiba, Zhepure, Tingri
36°N
Karakoram Fault
Ladakh
Kashmir
GCT
Zanskar
34°
Tibet, China
32°
74°E
Spiti
STDZ
(12)
(11)
Kailas
Dajin
0 100 200 km
30°
78°
(10)
Zhongba
Saga
Lhasa
Xigaze
MCT
MFT
(6-9)
(4, 5)
Tingri
GCT
Gyangze
(1-3)
Gamba
Qomo
28°N
MBT
Kathmandu
STDZ
MCT
82°
86°
90°
India
Gangdese batholith
Linzizong volcanic successions
Xigaze forearc strata
Yarlung-Zangbo ophiolites
Tethyan Himalaya
Greater Himalaya
Lesser Himalaya
Sub-Himalaya
Leucogranite
Mélange
Quaternary
Thrust
Normal fault
GCT - Great counter thrust
STDZ - South Tibet detachment zone
MCT - Main central thrust
MBT - Main boundary thrust

Fig. 2

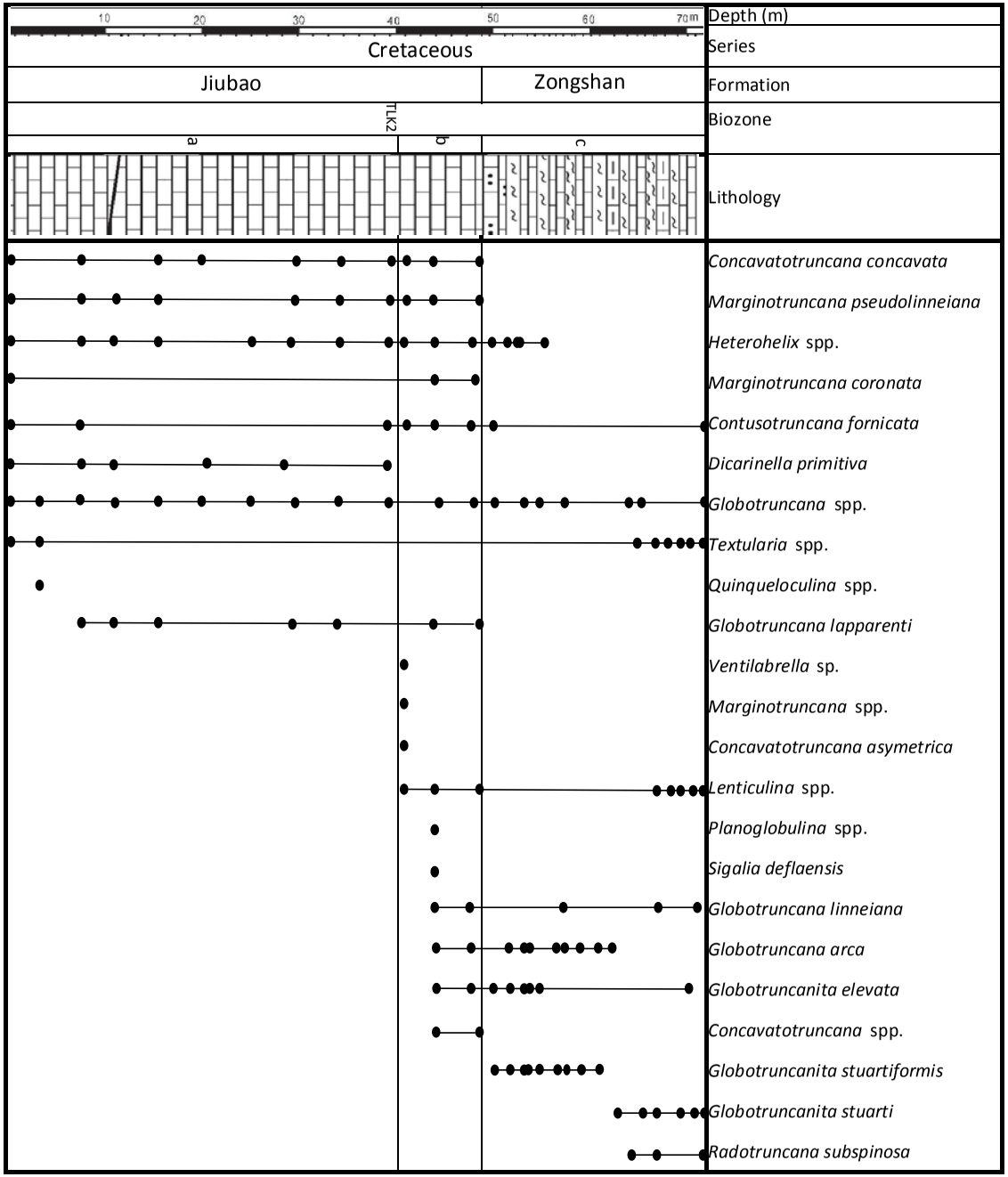
10
20
30
40
50
60
70m
Depth (m)
Cretaceous
Series
Jiubao
Zongshan
Formation
TLK2
Biozone
a
b
c
Lithology
Concavatotruncana concavata
Marginotruncana pseudolinneiana
Heterohelix spp.
Marginotruncana coronata
Contusotruncana fornicata
Dicarinella primitiva
Globotruncana spp.
Textularia spp.
Quinqueloculina spp.
Globotruncana lapparenti
Ventilabrella sp.
Marginotruncana spp.
Concavatotruncana asymetrica
Lenticulina spp.
Planoglobulina spp.
Sigalia deflaensis
Globotruncana linneiana
Globotruncana arca
Globotruncanita elevata
Concavatotruncana spp.
Globotruncanita stuartiformis
Globotruncanita stuarti
Radotruncana subspinosa

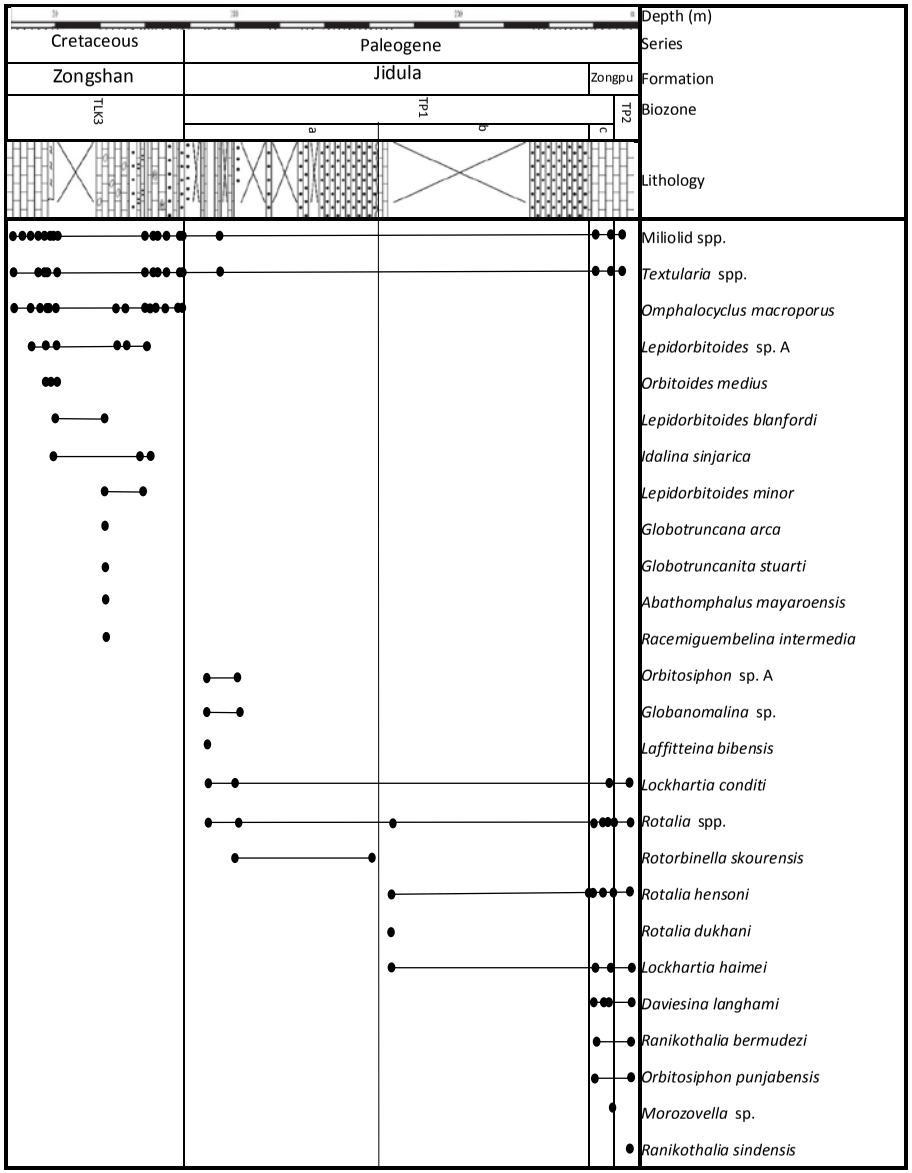
Depth (m)
Cretaceous
Paleogene
Series
Zongshan
Jidula
Zongpu
Formation
TLK3
TP1
TP2
a
b
c
Biozone
Lithology
Miliolid spp.
Textularia spp.
Omphalocyclus macroporus
Lepidorbitoides sp. A
Orbitoides medius
Lepidorbitoides blanfordi
Idalina sinjarica
Lepidorbitoides minor
Globotruncana arca
Globotruncanita stuarti
Abathomphalus mayaroensis
Racemiguembelina intermedia
Orbitosiphon sp. A
Globanomalina sp.
Laffitteina bibensis
Lockhartia conditi
Rotalia spp.
Rotorbinella skourensis
Rotalia hensoni
Rotalia dukhani
Lockhartia haimei
Daviesina langhami
Ranikothalia bermudezi
Orbitosiphon punjabensis
Morozovella sp.
Ranikothalia sindensis

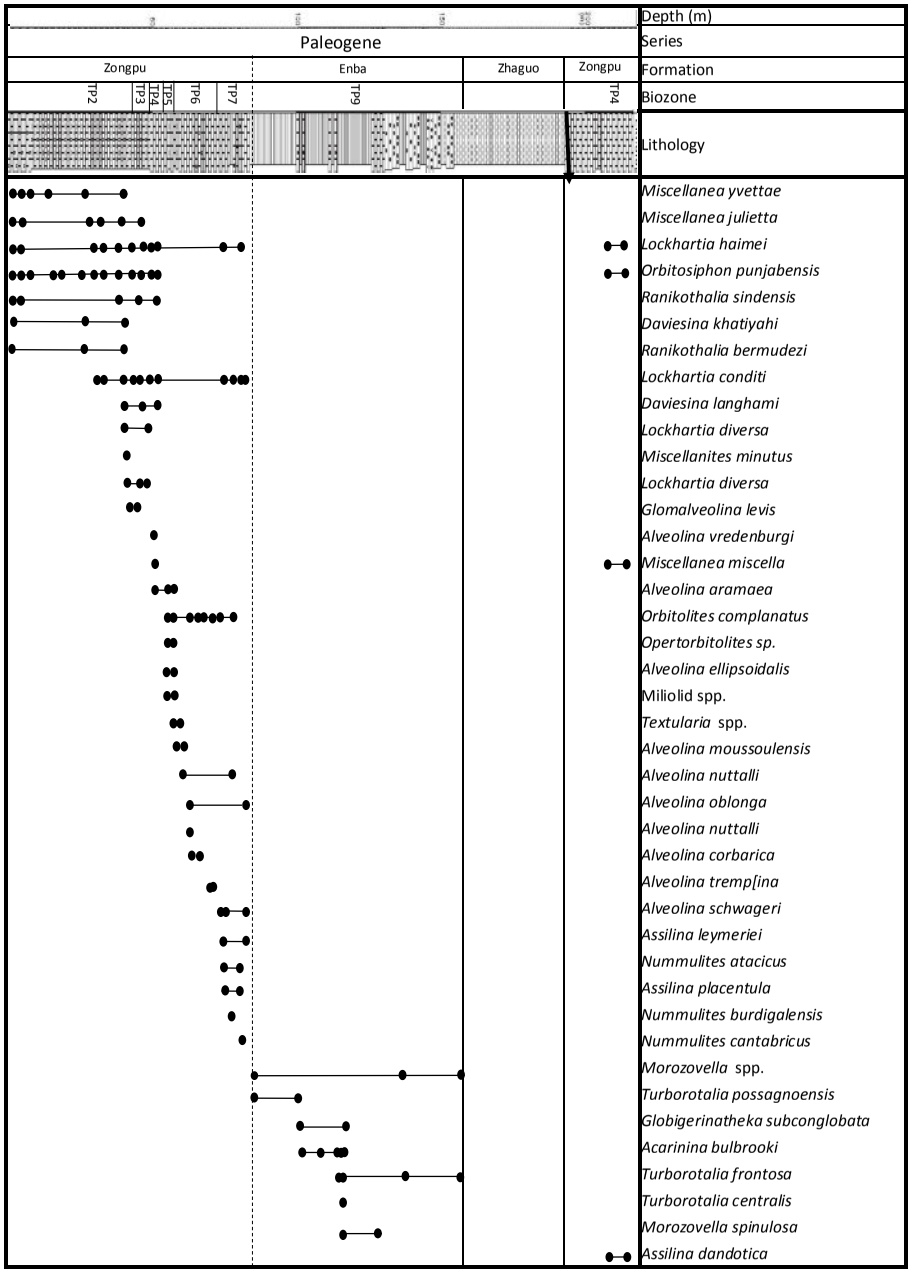
Depth (m)
Series
Paleogene
Formation
Zongpu
Enba
Zhaguo
Zongpu
Biozone
TP2
TP3
TP4
TP5
TP6
TP7
TP9
TP4
Lithology
Miscellanea yvettae
Miscellanea julietta
Lockhartia haimei
Orbitosiphon punjabensis
Ranikothalia sindensis
Daviesina khatiyahi
Ranikothalia bermudezi
Lockhartia conditi
Daviesina langhami
Lockhartia diversa
Miscellanites minutus
Lockhartia diversa
Glomalveolina levis
Alveolina vredenburgi
Miscellanea miscella
Alveolina aramaea
Orbitolites complanatus
Opertorbitolites sp.
Alveolina ellipsoidalis
Miliolid spp.
Textularia spp.
Alveolina moussoulensis
Alveolina nuttalli
Alveolina oblonga
Alveolina nuttalli
Alveolina corbarica
Alveolina trempʃina
Alveolina schwageri
Assilina leymeriei
Nummulites atacicus
Assilina placentula
Nummulites burdigalensis
Nummulites cantabricus
Morozovella spp.
Turborotalia possagnoensis
Globigerinatheka subconglobata
Acarinina bulbrooki
Turborotalia frontosa
Turborotalia centralis
Morozovella spinulosa
Assilina dandotica

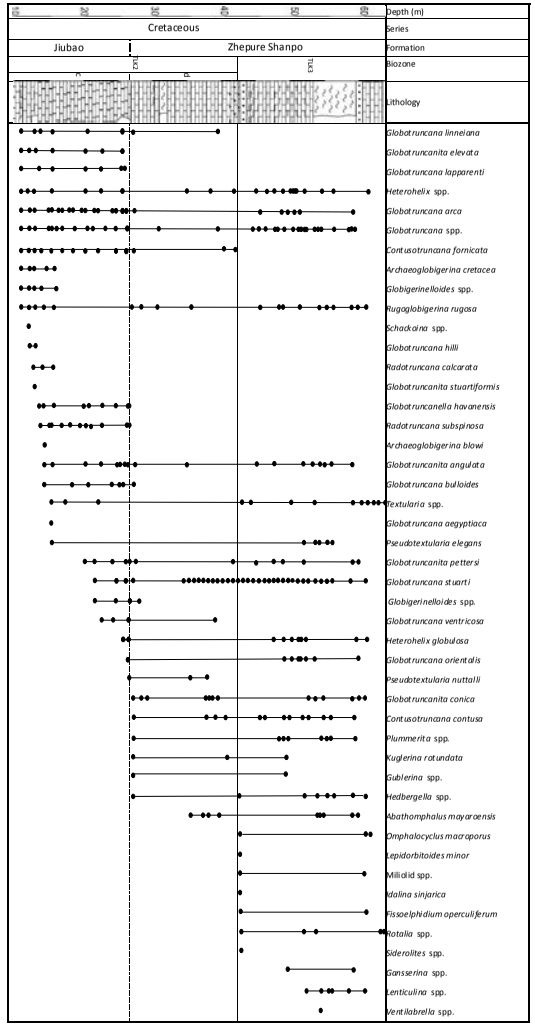
Depth (m)
Series
Cretaceous
Formation
Jiubao
Zhepure Shanpo
Biozone
EXTL
Lithology
Globotruncana linneiana
Globotruncanita elevata
Globotruncana lapparenti
Heterohelix spp.
Globotruncana arca
Globotruncana spp.
Contusotruncana fornicata
Archaeoglobigerina cretacea
Globigerinelloides spp.
Rugoglobigerina rugosa
Schackoina spp.
Globotruncana hilli
Radotruncana calcarata
Globotruncanita stuartiformis
Globotruncanella havanensis
Radotruncana subspinosa
Archaeoglobigerina blowi
Globotruncanita angulata
Globotruncana bulloides
Textularia spp.
Globotruncana aegyptiaca
Pseudotextularia elegans
Globotruncanita pettersi
Globotruncana stuarti
Globigerinelloides spp.
Globotruncana ventricosa
Heterohelix globulosa
Globotruncana orientalis
Pseudotextularia nuttalli
Globotruncanita conica
Contusotruncana contusa
Plummerita spp.
Kuglerina rotundata
Gublerina spp.
Hedbergella spp.
Abathomphalus mayaroensis
Omphalocyclus macroporus
Lepidorbitoides minor
Miliolid spp.
Idalina sinjarica
Fissoelphidium operculiferum
Rotalia spp.
Siderolites spp.
Gansserina spp.
Lenticulina spp.
Ventilabrella spp.

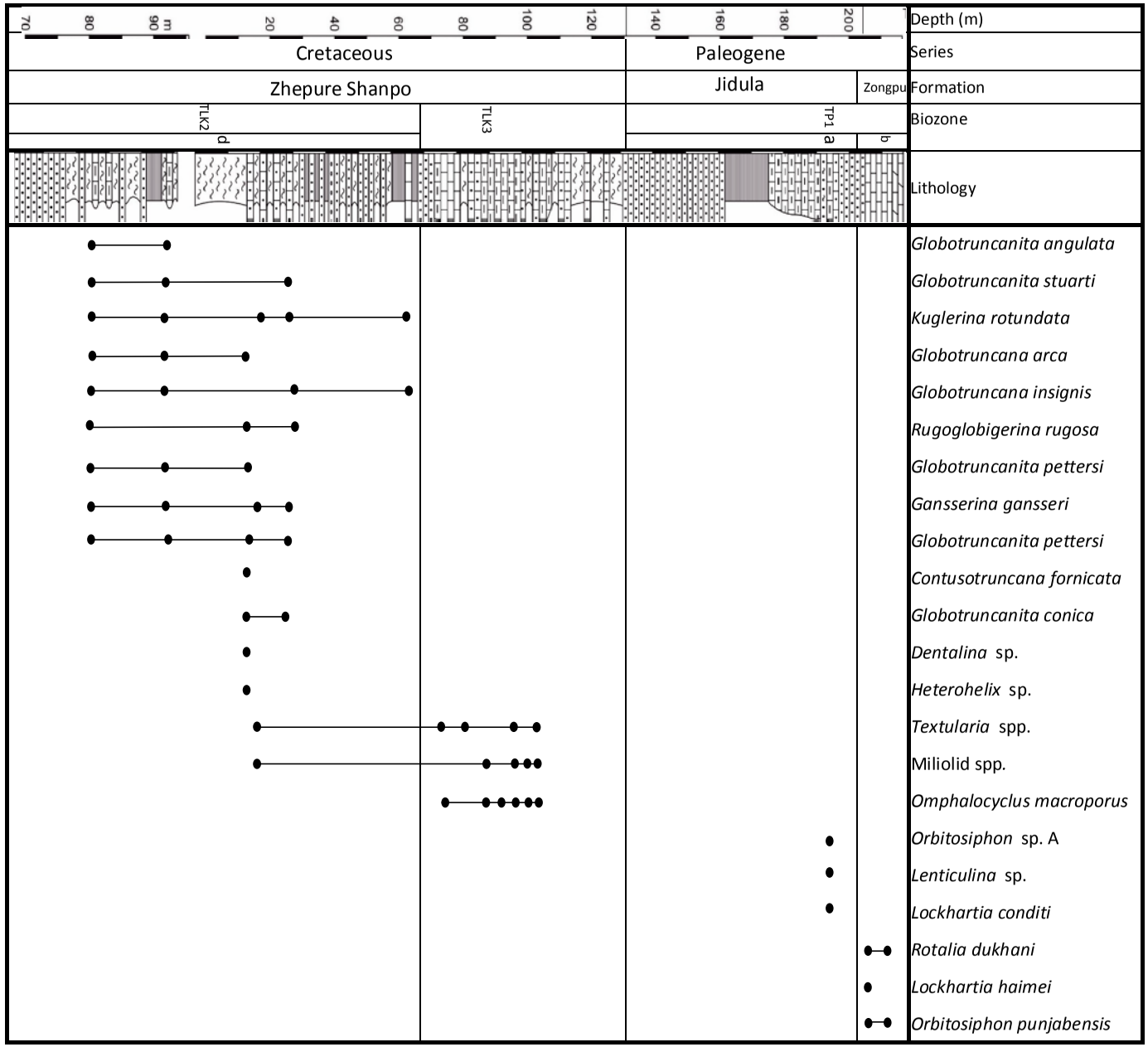
70
80
90
m
20
40
60
80
100
120
140
160
180
200
Depth (m)
Cretaceous
Paleogene
Series
Zhepure Shanpo
Jidula
Zongpu
Formation
TLK2
d
TLK3
TP1
a
b
Biozone
Lithology
Globotruncanita angulata
Globotruncanita stuarti
Kuglerina rotundata
Globotruncana arca
Globotruncana insignis
Rugoglobigerina rugosa
Globotruncanita pettersi
Gansserina gansseri
Globotruncanita pettersi
Contusotruncana fornicata
Globotruncanita conica
Dentalina sp.
Heterohelix sp.
Textularia spp.
Miliolid spp.
Omphalocyclus macroporus
Orbitosiphon sp. A
Lenticulina sp.
Lockhartia conditi
Rotalia dukhani
Lockhartia haimei
Orbitosiphon punjabensis

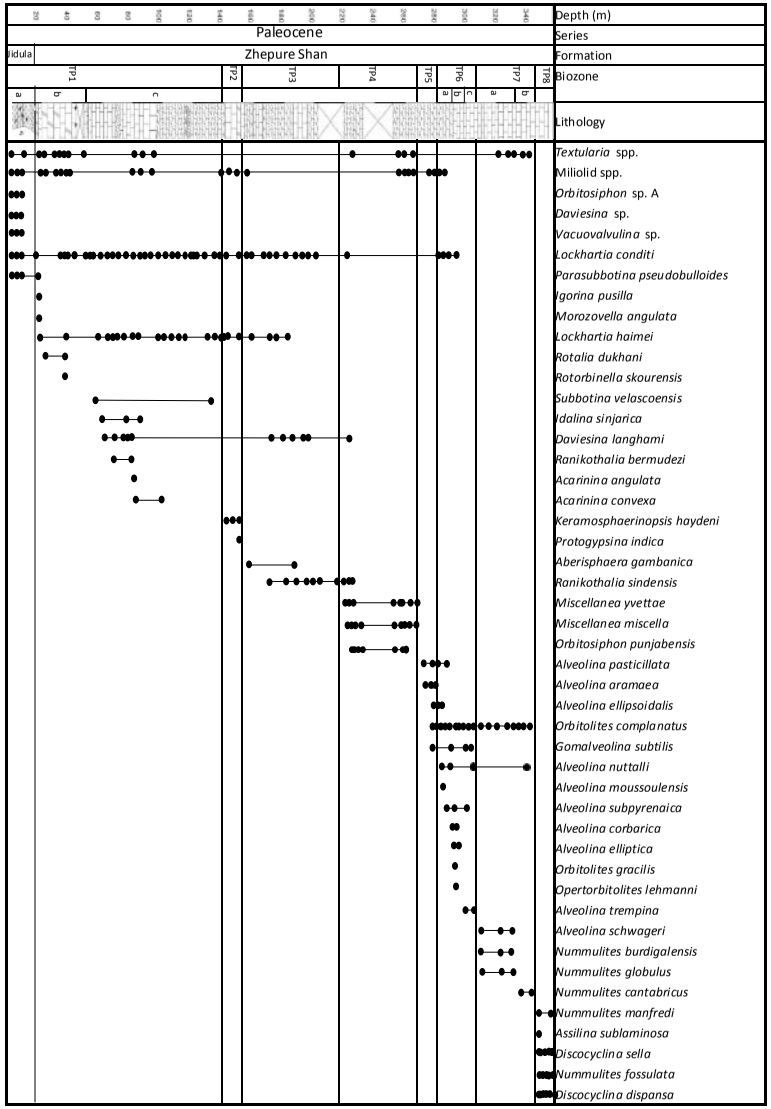
Depth (m)
Series
Paleocene
Formation
Zhepure Shan
Biozone
TP1
TP2
TP3
TP4
TP5
TP6
TP7
TP8
Lithology
Textularia spp.
Miliolid spp.
Orbitosiphon sp. A
Daviesina sp.
Vacuovalvulina sp.
Lockhartia conditi
Parasubbotina pseudobulloides
Igorina pusilla
Morozovella angulata
Lockhartia haimei
Rotalia dukhani
Rotorbinella skourensis
Subbotina velascoensis
Idalina sinjarica
Daviesina langhami
Ranikothalia bermudezi
Acarinina angulata
Acarinina convexa
Keramosphaerinopsis haydeni
Protogypsina indica
Aberisphaera gambanica
Ranikothalia sindensis
Miscellanea yvettae
Miscellanea miscella
Orbitosiphon punjabensis
Alveolina pasticillata
Alveolina aramaea
Alveolina ellipsoidalis
Orbitolites complanatus
Gomalveolina subtilis
Alveolina nuttalli
Alveolina moussoulensis
Alveolina subpyrenaica
Alveolina corbarica
Alveolina elliptica
Orbitolites gracilis
Opertorbitolites lehmanni
Alveolina trempina
Alveolina schwageri
Nummulites burdigalensis
Nummulites globulus
Nummulites cantabricus
Nummulites manfredi
Assilina sublaminosa
Discocyclina sella
Nummulites fossulata
Discocyclina dispansa


Depth (m)
Series
Paleogene
Formation
Zongpu
Enba
Biozone
Lithology
Orbitolites complanatus
Nummulites atacicus
Alveolina globosa
Nummulites globulus
Alveolina aragonensis
Assilina granulosa
Alveolina trempina
Assilina laminosa
Discocyclina ranikotensis
Nummulites mamillatus
Assilina leymeriei
Discocyclina dispansa
Nummulites cantabricus
Orbitosiphon punjabensis
Lockhartia conditi
Miscellanea julietta
Ranikothalia sp.
Daviesina langhami
Lockhartia haimei
Alveolina corbarica
Alveolina elliptica
Alveolina trempina
Nummulites burdigalensis
Nummulites cantabricus
Nummulites aturicus
Assilina papillata
Assilina plana
Nummulites manfredi
Turborotalia frontosa
Turborotalia pomeroli
Globigerinatheka curryi
Morozovella lehneri
Globigerinatheka barri
Acarinina spp.
Turborotalia possagnoensis

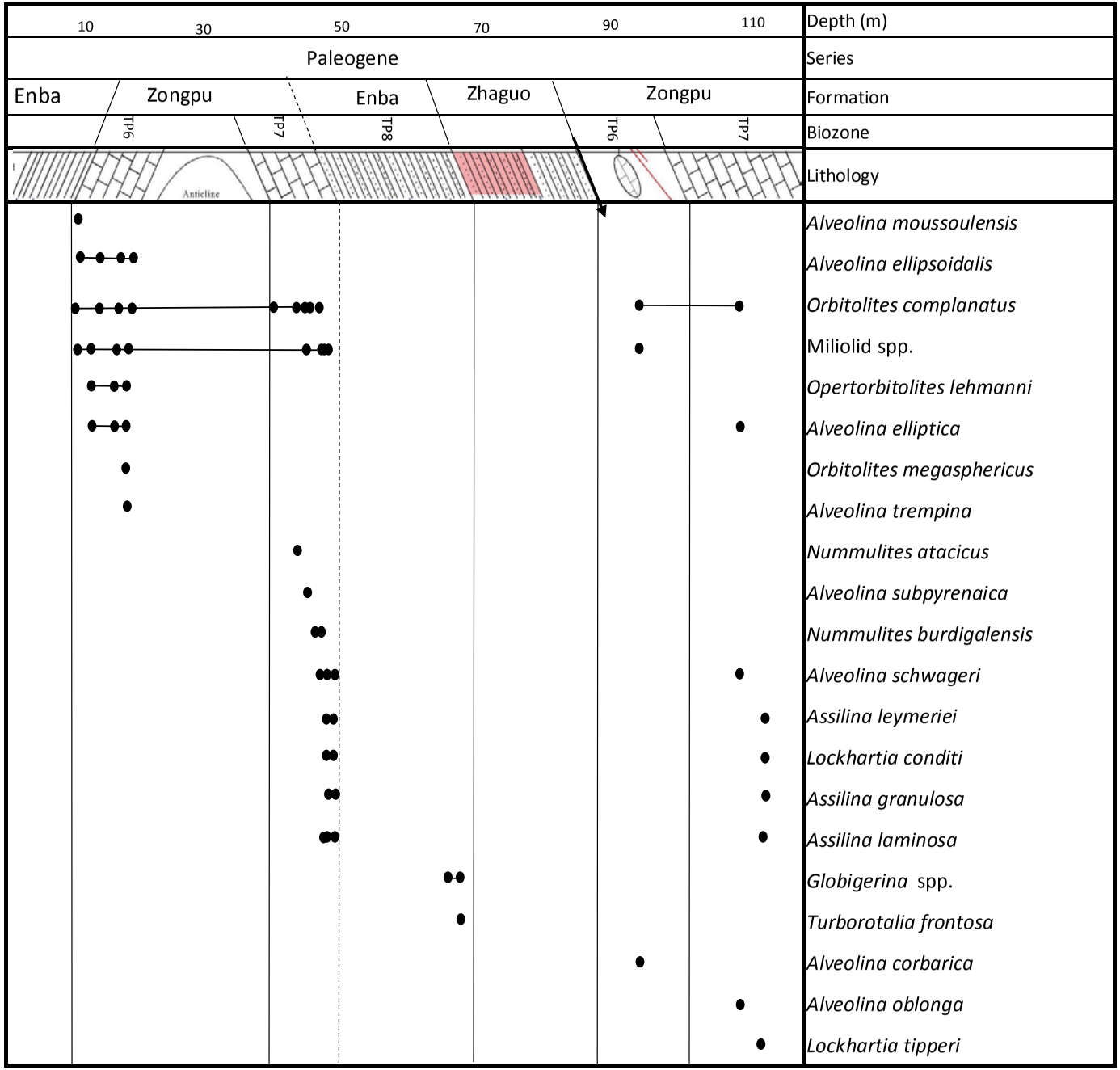
10
30
50
70
90
110
Depth (m)
Paleogene
Series
Enba
Zongpu
Enba
Zhaguo
Zongpu
Formation
TP6
TP7
TP8
TP6
TP7
Biozone
Antecline
Lithology
Alveolina moussoulensis
Alveolina ellipsoidalis
Orbitolites complanatus
Miliolid spp.
Opertorbitolites lehmanni
Alveolina elliptica
Orbitolites megasphericus
Alveolina trempina
Nummulites atacicus
Alveolina subpyrenaica
Nummulites burdigalensis
Alveolina schwageri
Assilina leymeriei
Lockhartia conditi
Assilina granulosa
Assilina laminosa
Globigerina spp.
Turborotalia frontosa
Alveolina corbarica
Alveolina oblonga
Lockhartia tipperi

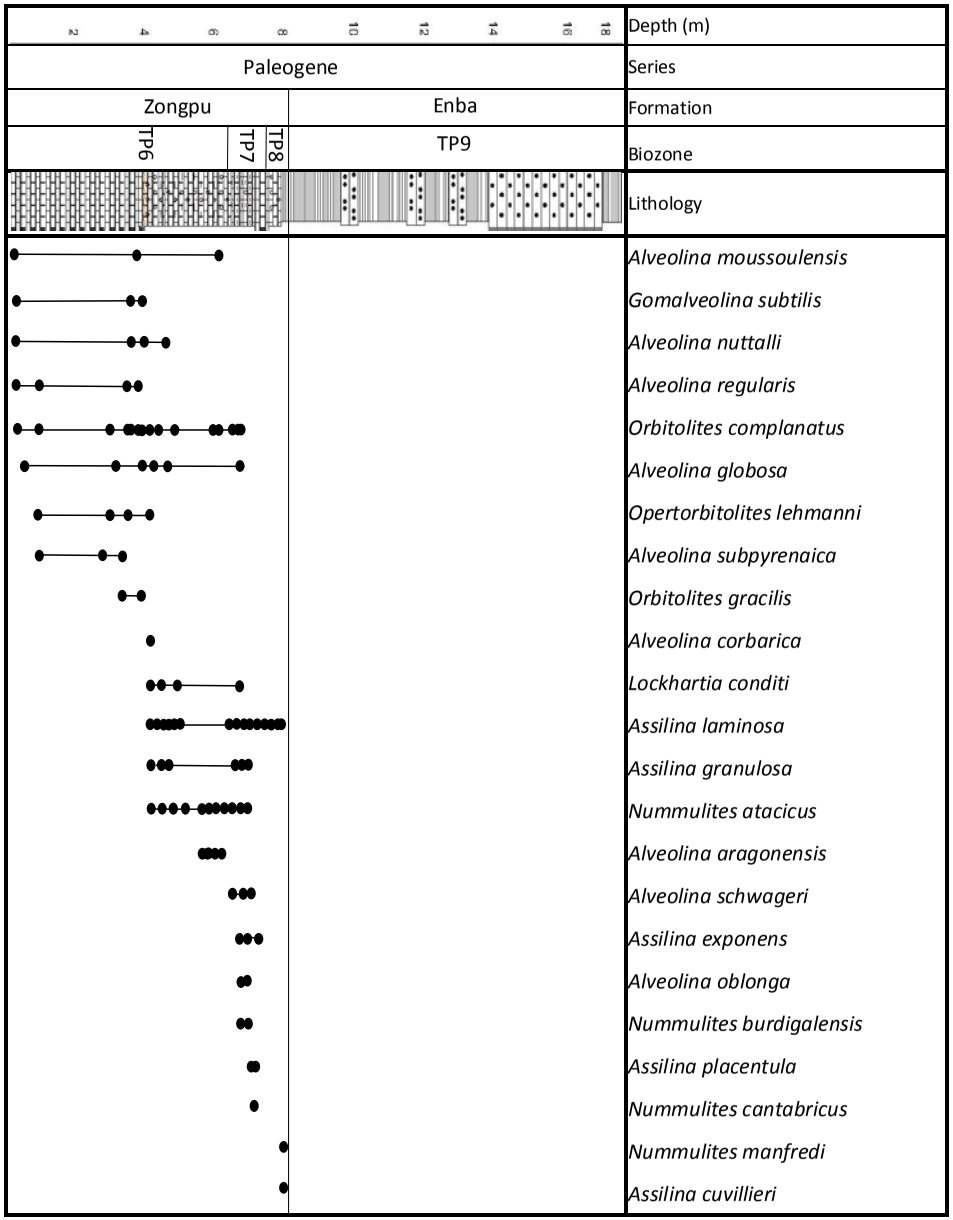
2
4
6
8
10
12
14
16
18
Depth (m)
Paleogene
Series
Zongpu
Enba
Formation
TP6
TP7
TP8
TP9
Biozone
Lithology
Alveolina moussoulensis
Gomalveolina subtilis
Alveolina nuttalli
Alveolina regularis
Orbitolites complanatus
Alveolina globosa
Opertorbitolites lehmanni
Alveolina subpyrenaica
Orbitolites gracilis
Alveolina corbarica
Lockhartia conditi
Assilina laminosa
Assilina granulosa
Nummulites atacicus
Alveolina aragonensis
Alveolina schwageri
Assilina exponens
Alveolina oblonga
Nummulites burdigalensis
Assilina placentula
Nummulites cantabricus
Nummulites manfredi
Assilina cuvillieri

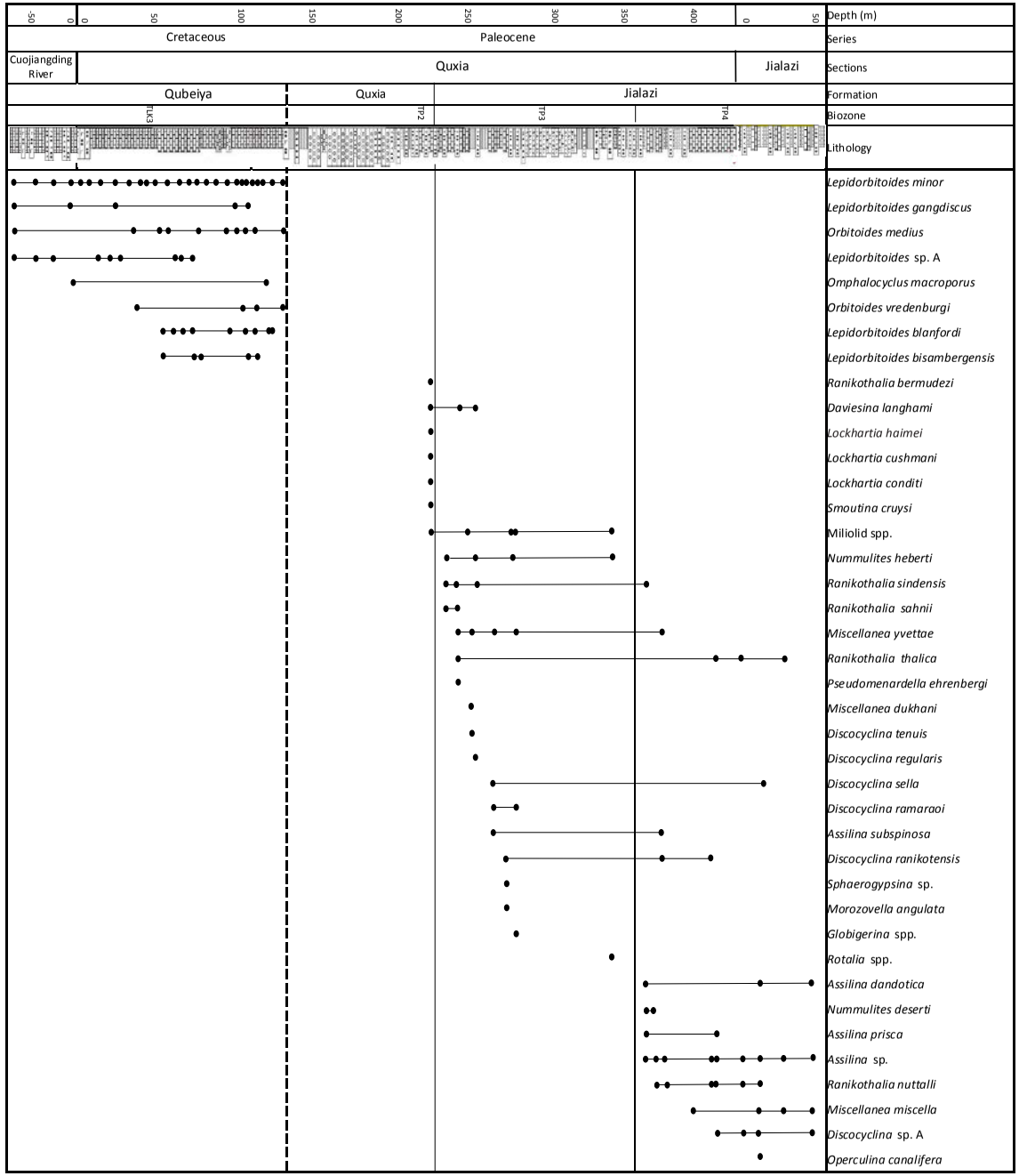
-50
0
0
50
100
150
200
250
300
350
400
0
50
Depth (m)
Cretaceous
Paleocene
Series
Cuojiangding River
Quxia
Jialazi
Sections
Qubeiya
Quxia
Jialazi
Formation
FLK3
FP2
FP3
FP4
Biozone
Lithology
Lepidorbitoides minor
Lepidorbitoides gangdiscus
Orbitoides medius
Lepidorbitoides sp. A
Omphalocyclus macroporus
Orbitoides vredenburgi
Lepidorbitoides blanfordi
Lepidorbitoides bisambergensis
Ranikothalia bermudezi
Daviesina langhami
Lockhartia haimei
Lockhartia cushmani
Lockhartia conditi
Smoutina cruysi
Miliolid spp.
Nummulites heberti
Ranikothalia sindensis
Ranikothalia sahnii
Miscellanea yvettae
Ranikothalia thalica
Pseudomenardella ehrenbergi
Miscellanea dukhani
Discocyclina tenuis
Discocyclina regularis
Discocyclina sella
Discocyclina ramaraoi
Assilina subspinosa
Discocyclina ranikotensis
Sphaerogypsina sp.
Morozovella angulata
Globigerina spp.
Rotalia spp.
Assilina dandotica
Nummulites deserti
Assilina prisca
Assilina sp.
Ranikothalia nuttalli
Miscellanea miscella
Discocyclina sp. A
Operculina canalifera

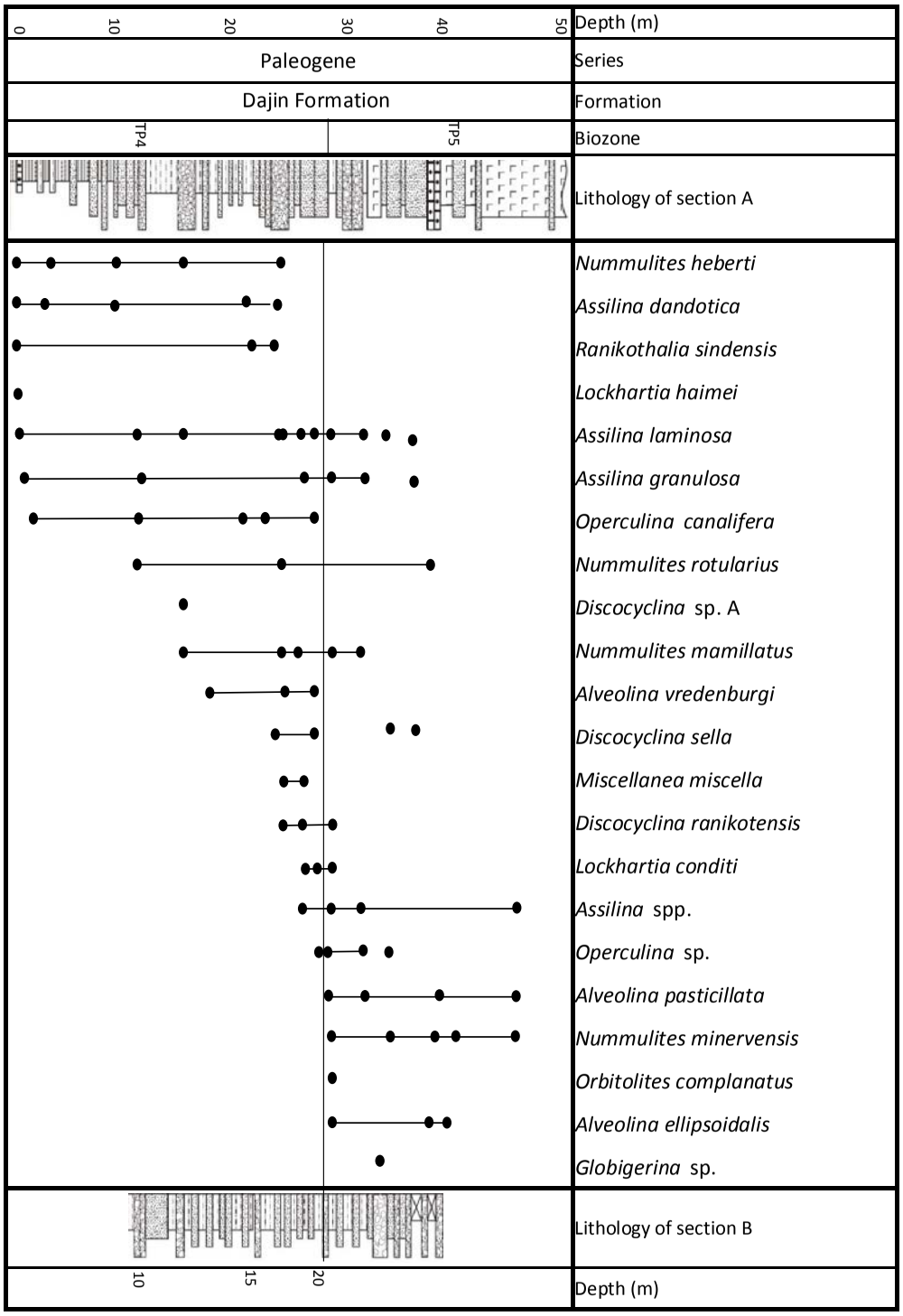
0
10
20
30
40
50
Depth (m)
Paleogene
Series
Dajin Formation
Formation
TP4
TP5
Biozone
Lithology of section A
Nummulites heberti
Assilina dandotica
Ranikothalia sindensis
Lockhartia haimei
Assilina laminosa
Assilina granulosa
Operculina canalifera
Nummulites rotularius
Discocyclina sp. A
Nummulites mamillatus
Alveolina vredenburgi
Discocyclina sella
Miscellanea miscella
Discocyclina ranikotensis
Lockhartia conditi
Assilina spp.
Operculina sp.
Alveolina pasticillata
Nummulites minervensis
Orbitolites complanatus
Alveolina ellipsoidalis
Globigerina sp.
Lithology of section B
10
15
20
Depth (m)

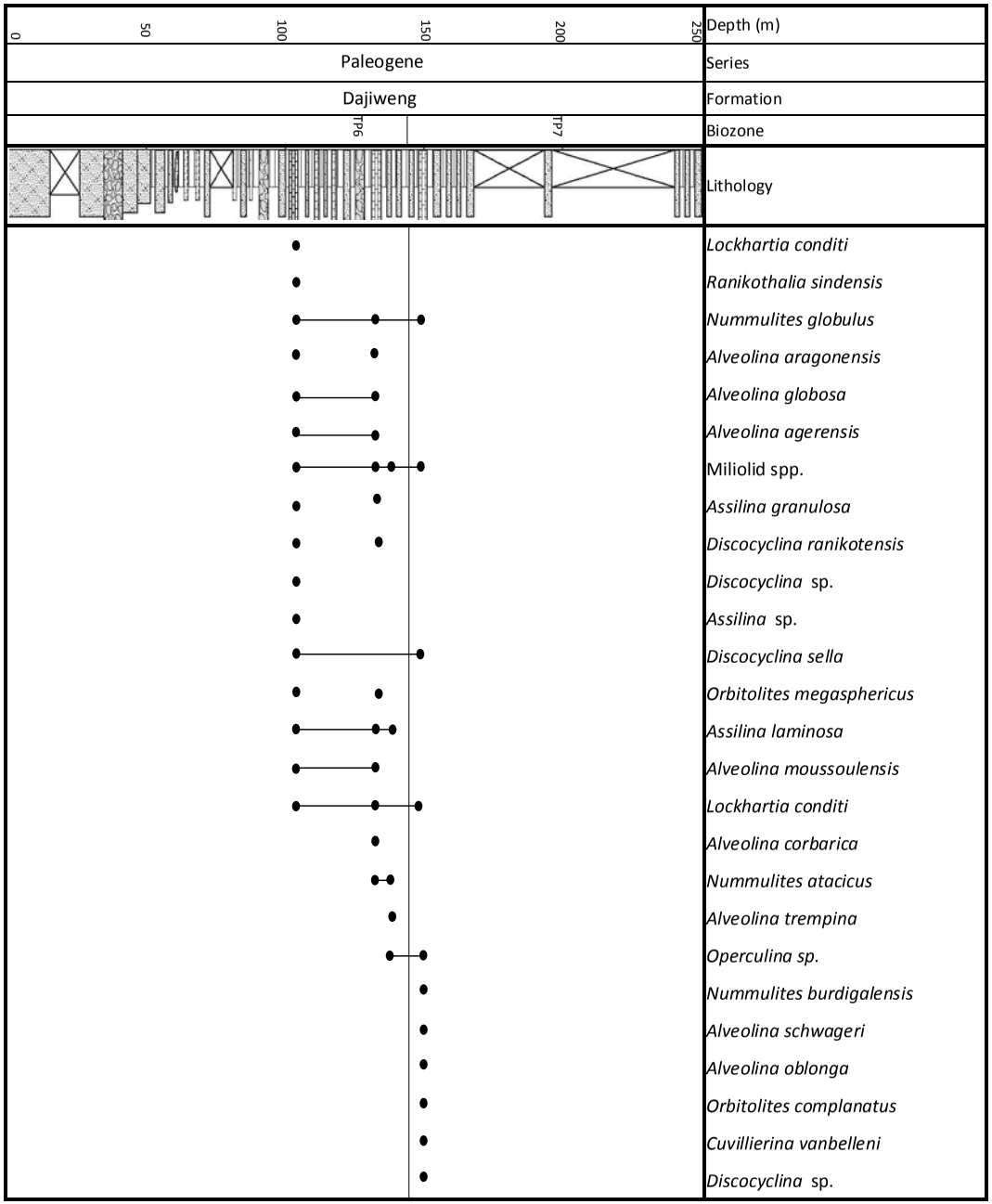
0
50
100
150
200
250
Depth (m)
Paleogene
Series
Dajiweng
Formation
TP6
TP7
Biozone
Lithology
Lockhartia conditi
Ranikothalia sindensis
Nummulites globulus
Alveolina aragonensis
Alveolina globosa
Alveolina agerensis
Miliolid spp.
Assilina granulosa
Discocyclina ranikotensis
Discocyclina sp.
Assilina sp.
Discocyclina sella
Orbitolites megasphericus
Assilina laminosa
Alveolina moussoulensis
Lockhartia conditi
Alveolina corbarica
Nummulites atacicus
Alveolina trempina
Operculina sp.
Nummulites burdigalensis
Alveolina schwageri
Alveolina oblonga
Orbitolites complanatus
Cuvillierina vanbelleni
Discocyclina sp.

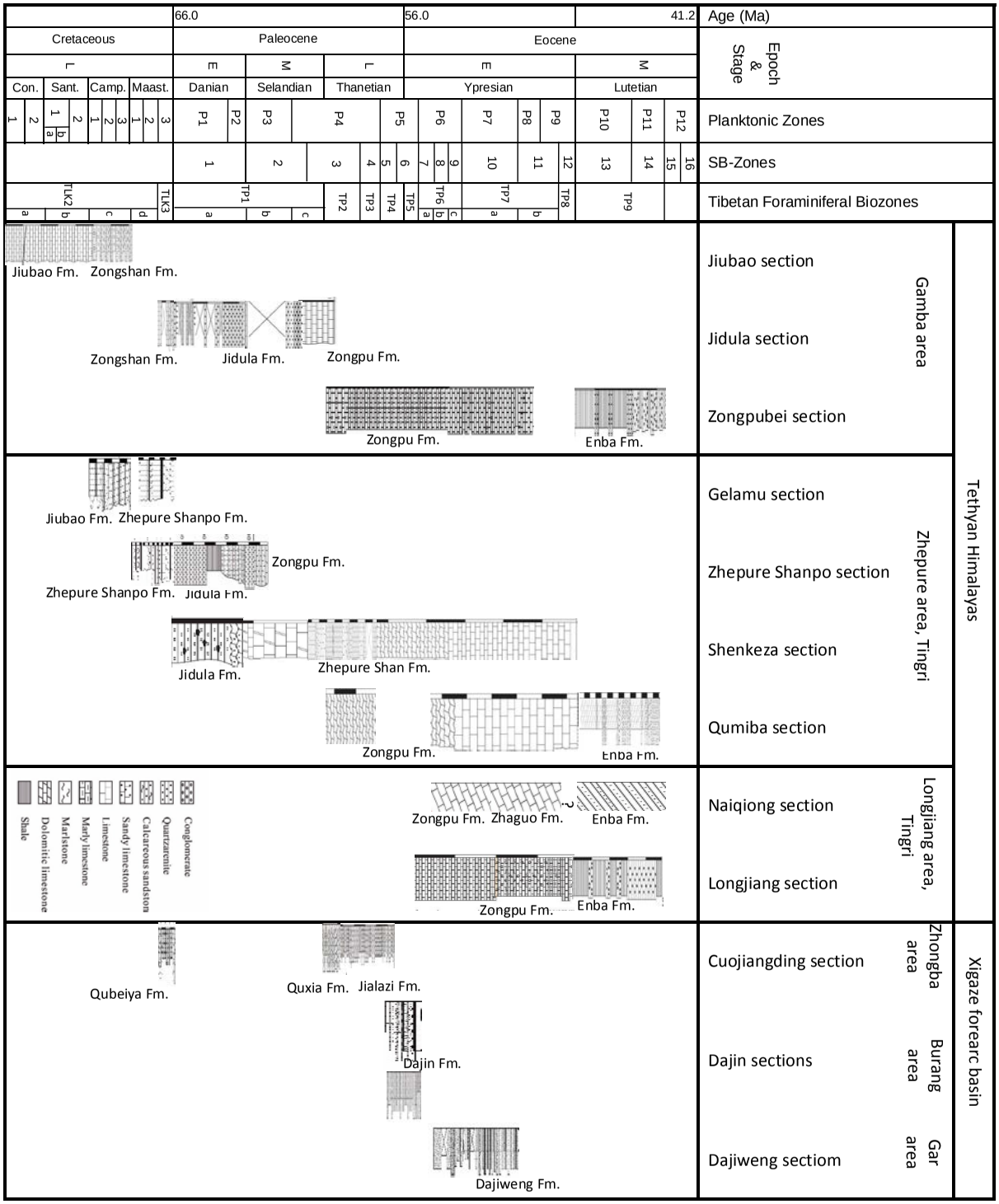
66.0
56.0
41.2
Age (Ma)
Cretaceous
Paleocene
Eocene
Epoch & Stage
L
E
M
L
E
M
Con.
Sant.
Camp.
Maast.
Danian
Selandian
Thanetian
Ypresian
Lutetian
Planktonic Zones
SB-Zones
Tibetan Foraminiferal Biozones
Jiubao Fm.
Zongshan Fm.
Jidula Fm.
Zongpu Fm.
Enba Fm.
Zhepure Shanpo Fm.
Zhepure Shan Fm.
Zhaguo Fm.
Shale
Dolomitic limestone
Marlstone
Marly limestone
Limestone
Sandy limestone
Calcareous sandston
Quartzarenite
Conglomerate
Qubeiya Fm.
Quxia Fm.
Jialazi Fm.
Dajin Fm.
Dajiweng Fm.
Jiubao section
Jidula section
Zongpubei section
Gamba area
Gelamu section
Zhepure Shanpo section
Shenkeza section
Qumiba section
Zhepure area, Tingri
Naiqiong section
Longjiang section
Longjiang area, Tingri
Cuojiangding section
Zhongba area
Dajin sections
Burang area
Dajiweng sectiom
Gar area
Tethyan Himalayas
Xigaze forearc basin

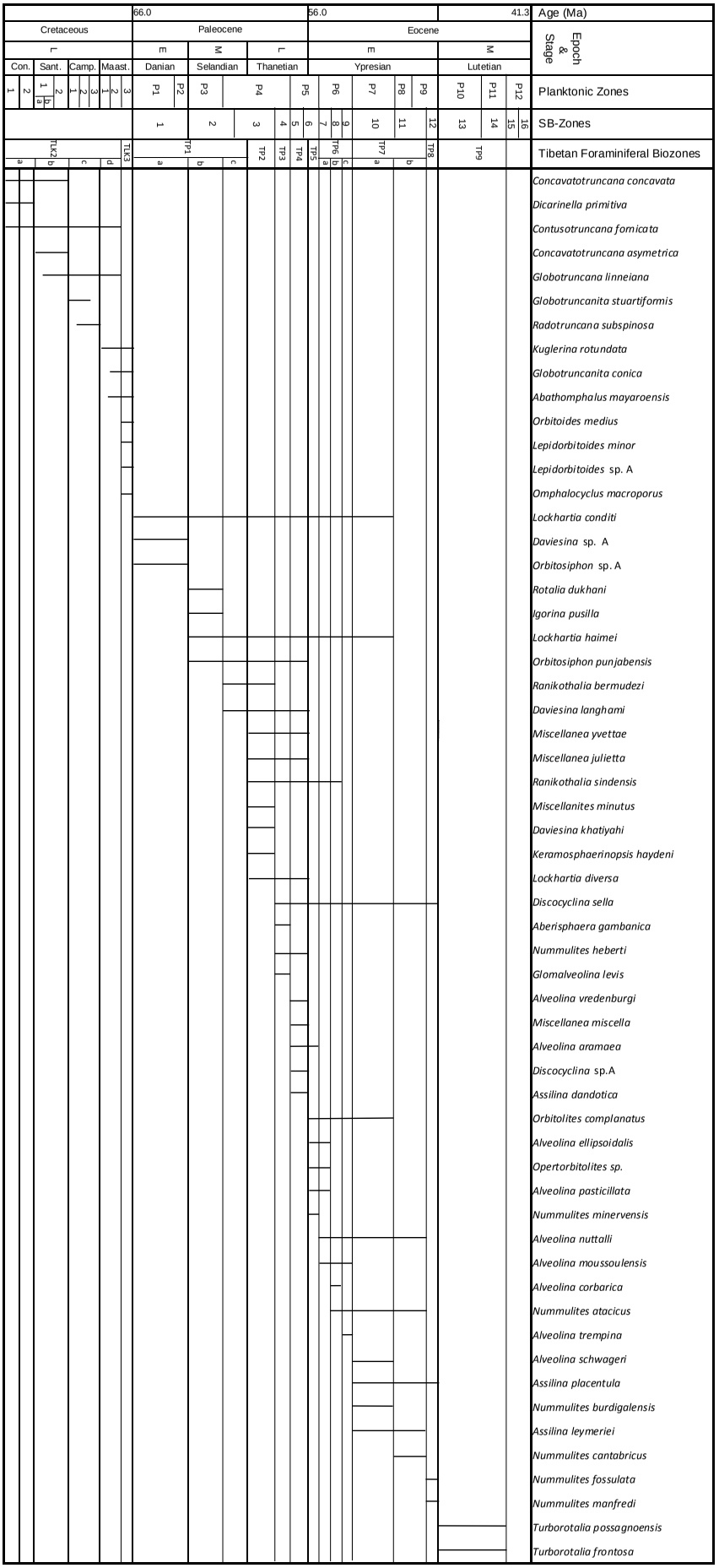
66.0
56.0
41.3
Age (Ma)
Cretaceous
Paleocene
Eocene
Epoch & Stage
L
E
M
L
E
M
Con.
Sant.
Camp.
Maast.
Danian
Selandian
Thanetian
Ypresian
Lutetian
Planktonic Zones
SB-Zones
Tibetan Foraminiferal Biozones
Concavatotruncana concavata
Dicarinella primitiva
Contusotruncana fornicata
Concavatotruncana asymetrica
Globotruncana linneiana
Globotruncanita stuartiformis
Radotruncana subspinosa
Kuglerina rotundata
Globotruncanita conica
Abathomphalus mayaroensis
Orbitoides medius
Lepidorbitoides minor
Lepidorbitoides sp. A
Omphalocyclus macroporus
Lockhartia conditi
Daviesina sp. A
Orbitosiphon sp. A
Rotalia dukhani
Igorina pusilla
Lockhartia haimei
Orbitosiphon punjabensis
Ranikothalia bermudezi
Daviesina langhami
Miscellanea yvettae
Miscellanea julietta
Ranikothalia sindensis
Miscellanites minutus
Daviesina khatiyahi
Keramosphaerinopsis haydeni
Lockhartia diversa
Discocyclina sella
Aberisphaera gambanica
Nummulites heberti
Glomalveolina levis
Alveolina vredenburgi
Miscellanea miscella
Alveolina aramaea
Discocyclina sp.A
Assilina dandotica
Orbitolites complanatus
Alveolina ellipsoidalis
Opertorbitolites sp.
Alveolina pasticillata
Nummulites minervensis
Alveolina nuttalli
Alveolina moussoulensis
Alveolina corbarica
Nummulites atacicus
Alveolina trempina
Alveolina schwageri
Assilina placentula
Nummulites burdigalensis
Assilina leymeriei
Nummulites cantabricus
Nummulites fossulata
Nummulites manfredi
Turborotalia possagnoensis
Turborotalia frontosa

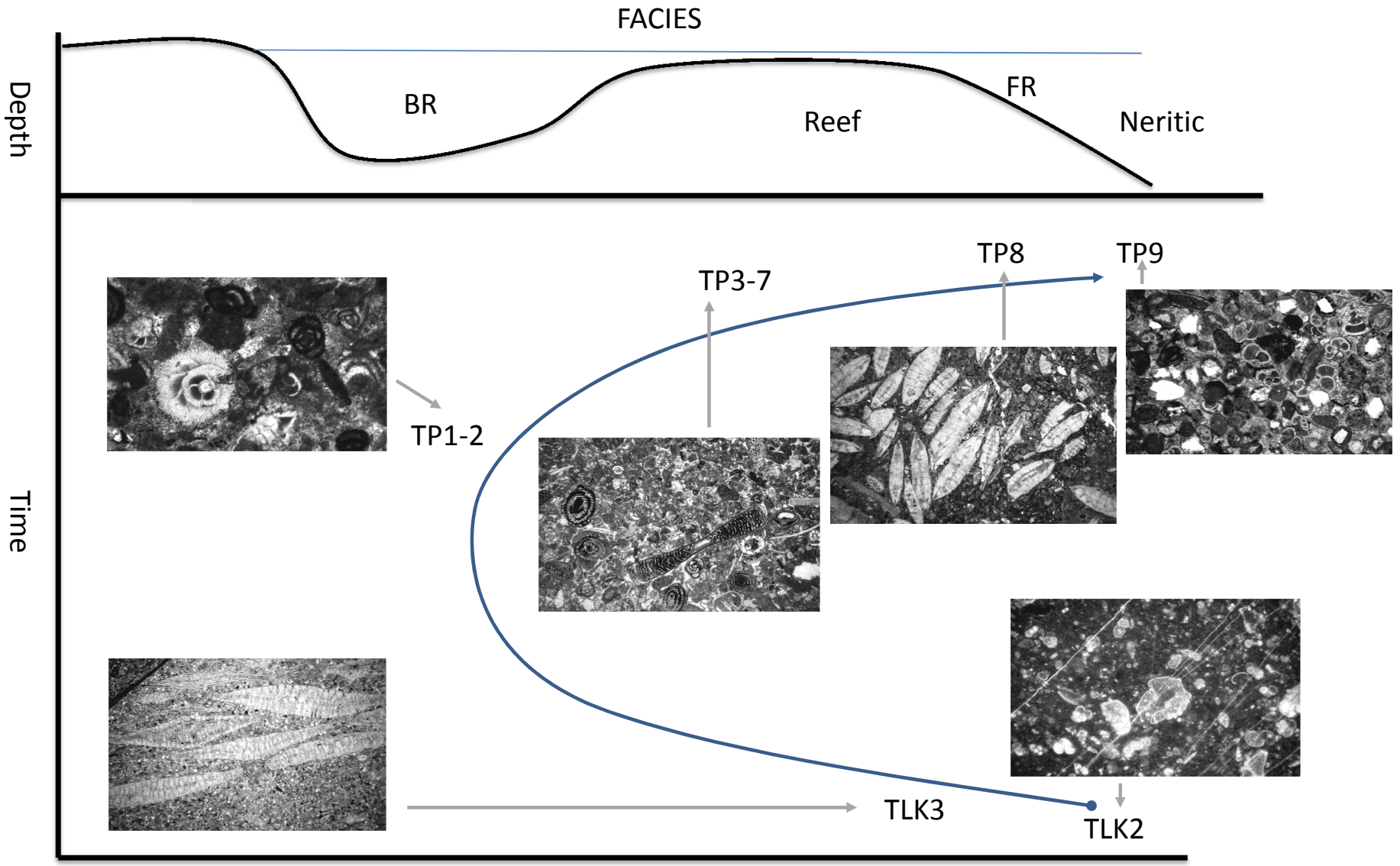
FACIES
Depth
BR
Reef
FR
Neritic
Time
TP1-2
TP3-7
TP8
TP9
TLK3
TLK2

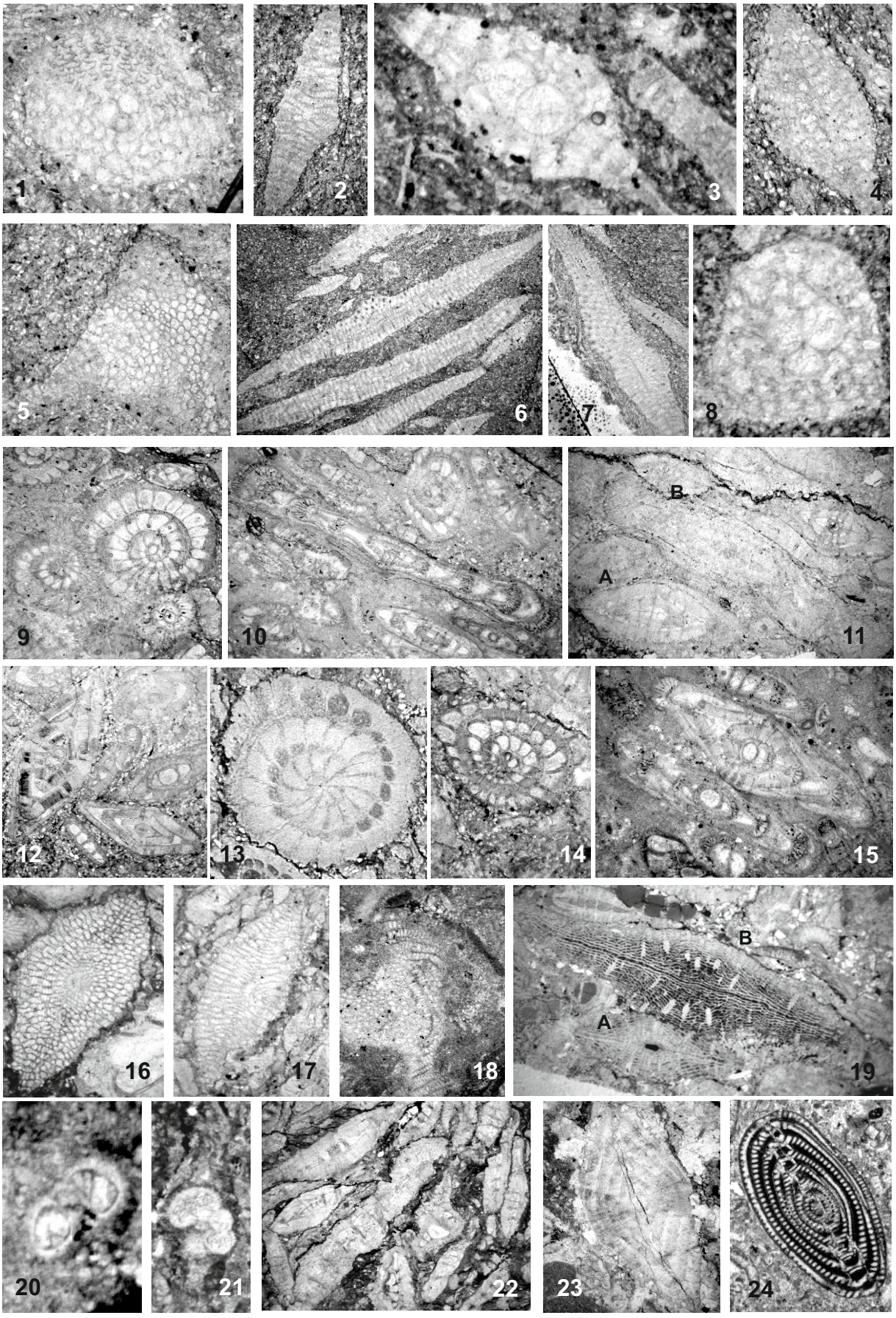
1
2
3
4
5
6
7
8
9
10
B
A
11
12
13
14
15
16
17
18
B
A
19
20
21
22
23
24

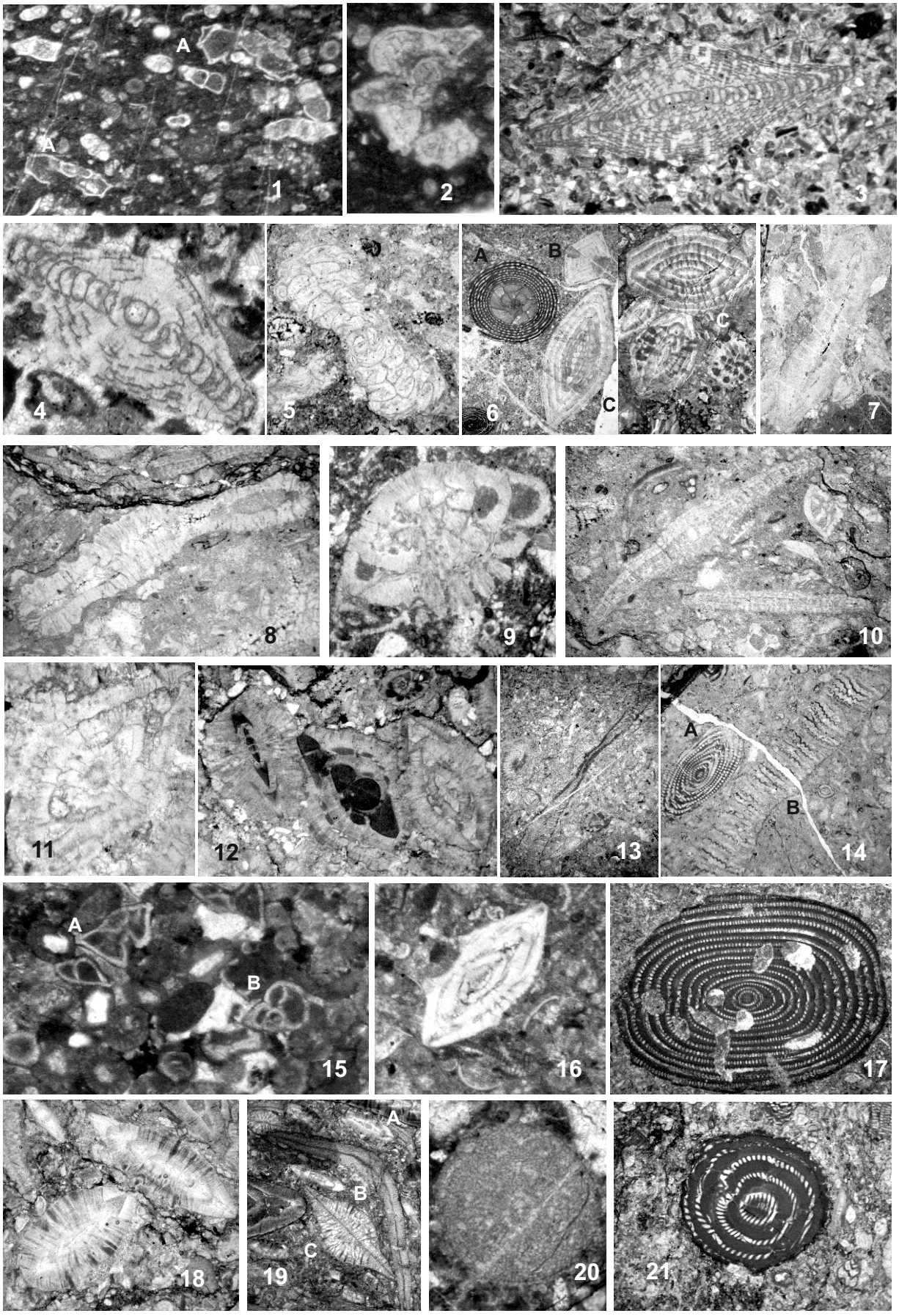
A
A
1
2
3
4
5
A
B
C
6
C
7
8
9
10
11
12
13
A
B
14
A
B
15
16
17
18
A
B
C
19
20
21